

## Manuscript Details

<b>Manuscript number</b>	MICROC_2019_3363_R1
<b>Title</b>	Geochemical and petrographic assessment of clay outcrops and archaeological ceramics from the pre-Hispanic site of Aguas Buenas (cal 400 -1250 CE), central Nicaragua
<b>Article type</b>	Research Paper

### Abstract

This research characterizes and reconstructs clay procurement and production practices through the integration of in-situ portable XRF and petrographic analysis on ancient ceramics and clay materials recovered from the Mayales river subbasin (central Nicaragua). A particular choice for this study was the largest and arguably most significant archaeological site in the area, Aguas Buenas (cal 400–1250 CE), a pre-Hispanic indigenous agglomeration consisting of 371 human-made mounds of various shapes arranged in geometric patterns. Microanalytical approaches were applied to reconstruct the use of raw mineral resources in the production of ubiquitous pottery materials found at this site and in its immediate surroundings. The resulting compositional analysis produced geochemical and mineralogical data allowing for the characterisation of distinct, geologically-based compositional groups throughout the valley, improving on the limited geological data resolution previously available. The integrated microscopic and compositional analysis (through p-XRF) of archaeological pottery materials and raw clay samples, generates a number of hypotheses and insights about the nature of the Aguas Buenas site, and its role as a shared space among groups living in the Mayales river subbasin. Additionally, this study provides a solid research framework of investigation that can be employed for more detailed and extensive future studies on pre-Hispanic human occupation in this research area or elsewhere.

<b>Keywords</b>	Archaeological provenance; pre-Hispanic Nicaragua; Petrography; Ceramic microstructure; Geochemical analysis
<b>Manuscript category</b>	Atomic Spectroscopy
<b>Corresponding Author</b>	Simone Casale
<b>Order of Authors</b>	Simone Casale, Natalia R. Donner, Dennis Braekmans, Alexnder Geurds

## Submission Files Included in this PDF

### File Name [File Type]

Cover letter.docx [Cover Letter]

Response to reviewers.docx [Response to Reviewers]

Highlights.docx [Highlights]

Manuscript .docx [Manuscript File]

Figure 1.pdf [Figure]

Figure 2.pdf [Figure]

Figure 3.pdf [Figure]

Figure 4.pdf [Figure]

Table1.docx [Table]

Table 2.docx [Table]

Table3.docx [Table]

Table 4.docx [Table]

declaration-of-competing-interests.docx [Conflict of Interest]

Credit author Statement.docx [Author Statement]

Supplementary tables.docx [Supplementary Material]

To view all the submission files, including those not included in the PDF, click on the manuscript title on your EVISE Homepage, then click 'Download zip file'.

FACULTY OF ARCHAEOLOGY  
LEIDEN UNIVERSITY  
EINSTEINWEG 2, 2333 CC LEIDEN  
THE NETHERLANDS



— February 27th, 2020

Dear Editor,

— Thank you very much for reviewing our manuscript “Geochemical and petrographic assessment of clay outcrops and archaeological ceramics from the pre-Hispanic site of Aguas Buenas (cal 400 -1250 CE), central Nicaragua”. The suggestions offered by the reviewers have been very helpful, enabling us to make significant improvements. We have carried out the changes the reviewers suggested and revised the manuscript accordingly.

— The systematic changes to our manuscript, based on the comments of the reviewers, have been marked in the submitted revised manuscript. We have also attached a document with our detailed responses to each of the comments of all reviewers.

We hope this revision meets all requirements for your consideration and we are looking forward to receiving your response.

Sincerely yours,

Simone Casale, Dennis Braekmans, Natalia Donner, Alexander Geurds

**MR. SIMONE CASALE**  
Faculty of Archaeology  
Leiden University  
Einsteinweg 2, 2333 CC Leiden  
The Netherlands  
casale@kitlv.nl

### **Responses to suggestions and remarks from reviewers:**

Dear Editor, Reviewers,

We would like to thank you for taking the time to provide a thorough review in order to further improve the quality of this manuscript. We have addressed all the points raised, which are detailed in blue in this response below and marked in the paper in red.

We hope this revision meets all requirements and look forward to receiving your response.

Best wishes,

Simone Casale, Natalia Donner, Dennis Braekmans and Alexander Geurds

Comments from the editors and reviewers:

#### **-Reviewer 1**

This is an interesting work with meaningful conclusion. Yet it is in fact a first framework of investigation as authors mention: "first framework of investigation that can be employed in future extensive studies on the Mayales river subbasin, and the chosen methodology holds potential for its application in other regions as well. It is likely that additional systematic and large-scale archaeometric analysis based on, for example, more high-resolution compositional techniques (such as for example INAA and ICP-MS), applied to cultural materials from sites spanning the entire subbasin, will further clarify the extent of connectivity between groups in central Nicaragua.". However, its worth publishing. Nevertheless there are some points that should be addressed.

Authors refer to the "Macro-fabric analysis" but actually this is not defined or presented in a sufficient way.

In order to clarify the macro-fabric analysis we elaborated more on sample description, adding more data on firing technology, the disposition of the mineral inclusions and voids and technological insights. We now consider that this additional data provides an expanded overview of the ceramic preparation and production, as based on macroscopic observations.

Do avoid statements like "about"... "About 2% of the sherd" (line 278 pp5)

We removed "about" from the sentence since the sample set selected represents 2% of the available assemblage.

The legends of the images must allow an easy "immediate" interpretation of the figures/graphs. On fig 3 replace Ca by Calcium, and,... (Also do include the unit used and hopefully also the uncertainties of the measures).

We changed the description of the images for the scatterplots throughout the text and we added a table (Table 3) where the standard deviation values for each group are reported.

I suggest considering and discuss even if just in a "future work" perspective, image characterization technics and rugometric and microtopographic inspection and analysis of ceramics' surfaces

We agree that image characterization techniques might offer an alternative interesting view for the analysis of the ceramics' surfaces, but we refrained from utilizing this here. As a next analytical phase we would rather initially focus on XRD for detailed mineral analysis to further specify firing temperatures.

## -Reviewer 2

The manuscript describes a geochemical and petrographic study of archaeological ceramics and clays from the pre-Hispanic site of Aguas Buenas in central Nicaragua. Geochemical measurements for a number of elements were made using a portable XRF spectrometer. Principal components analysis (PCA) was used to identify groups within the assemblage.

Although the manuscript has potential, there are a number of problems that the authors need to address.

We have addressed systematically the suggestions and remarks raised in order to improve the paper regarding clarity and data interpretation.

### 1. References cited section is missing from the manuscript.

Without seeing the references it is not possible to determine if the authors did a thorough search of the literature before writing this article.

The references appeared indeed apparently outside of the manuscript but we assume was a problem with the format for uploading the documents. Naturally, a full reference list is included in the manuscript.

### 2. The description of XRF contains some inaccuracies and is incomplete.

XRF is one of many techniques capable of providing compositional analysis of materials such as pottery and clays. There are two primary methods of XRF. These are Energy Dispersive XRF and Wavelength Dispersive XRF. The most common type of XRF is ED-XRF and it can be performed using either lab-based or portable XRF spectrometer non-destructively. WD-XRF does involve sample destruction. Other than the fact that the portable XRF can be easily transported from place to place, a lab-based XRF spectrometer and portable XRF spectrometer have no difference.

We agree with reviewer 2. There are indeed two types of XRF (ED-XRF and WD-XRF) and in the previous version of the paper, this aspect was perhaps not clarified enough. Following the suggestions provided, we improved the Material and Methods section and we further detailed how the methodology was applied and with what rationale.

According to the manuscript the authors used a filter that enhanced the mid-Z trace elements (Rb, Sr, Y, Zr, and Nb). A number of other elements were also measured, including K, Ca, Ti, Ba, Cr, Fe, Ni, and Zn. However, Tables 2 and 3 fail to list all of the elements consistently. Cr is present in one table but not the other. I also find strange their claim that Rb was not well measured, because it is usually one of the most reliable elements for measurement by XRF.

I recommend that the authors include a supplementary table listing all of the elemental data.

We have included a revised and complete table, in order to show the entire compositional spectrum. Cr was not included in table 3 because it was not considered for PCA analysis, however following the suggestion of the review, Cr was included in the table. Rb was erroneously not present in the table but an updated table with all quantified elemental data and text has been added to the manuscript.

The authors mention that several certified reference materials were measured for quality control. The QC results for some of these materials should be included in the paper to prove the data are accurate.

A table of measured versus certified reference materials has been added to the manuscript as supplementary material.

### 3. Discussion of data interpretation contains inaccuracies about PCA.

I am disappointed in some of the statements used to describe data interpretation.

The authors mention two types of plots (bivariate and biplots). [Personally, I prefer to use the term scatterplot instead of bivariate plot, but that is not the issue here.] Both type of plots are two-dimensional. However, a biplot is a special type of plot created using following principal components analysis (PCA) showing two different types of information. The information on a biplot should show both the principal component scores for all samples and vectors indicating the directions and magnitudes of elements describing differences between samples. Because the authors only plotted scores, their “biplot” is actually a bivariate plot of PC1 versus PC2. The authors should read the original articles by Neff (1994) to understand the distinction.

Neff (1994). RQ-mode principal components analysis of ceramic compositional data. *Archaeometry* 36(1): 115-130.

Thank you for this constructive clarification. The naming of the plots have been systematically revised throughout the text.

-A second problem with the authors' description of PCA is their statement in line 250 that the PCA allows reducing the data to two dimensions. This is incorrect. According to their description, they used eight elements (K, Fe, Ca, Ti, Cr, Nb, Sr, and Zr) in their PCA. The PCA will produce eight principal components not two. What actually happens is that the PCA has constructed a new space in which the first few components contain the most information about variation in the 8-element dataset. Thus, it is often true that PC1 versus PC2 are one of the best plots to examine. However, there is still potential for information in PC1 versus PC3, PC2 versus PC3, etc.

We agree with the comment raised here and expanded/clarified this in the text. A PC1 vs PC2 plot is indeed not the only data that can be retrieved, but in this case, as mostly in this type of studies, carry as expected the most information. We added the values of PC1 and PC2 to the text and to the graph, together with the values of the elements in the table. We believe that now the text and the graph provide suitable information for the correct interpretation of the data.

A third problem is how did they construct the ellipses on the PC plot. Were they calculated at some confidence interval (e.g. 90%) or are these just estimates?

My final criticism is related to one above. Also as part of line 250, the authors claim that they used the two-dimensional PCA plot to verify the groups established by petrography. The plot supports the groups but it does not verify or validate the groups. To validate the groups, one needs to use a method that performs a probability assessment. For instance, one dimensional data use the well known student's t-test. For multivariate data one should calculate probabilities using Mahalanobis Distances.

Following the points raised by the reviewer, discriminant analysis was selected to validate the identified groups after petrographic observation and the PCA analysis. The results of the Discriminant Analysis using Mahalanobis distances demonstrate that in both cases almost 80% of the samples were assigned to the same groups identified with the petrographic observation and PCA analysis, largely validating the grouping and offering areas to discuss.

I think this manuscript needs some serious rewriting before it will be acceptable for publication.

We would like to thank Reviewer 2 for the critical and constructive comments provided allowing us to improve the manuscript.

- (late extra) Reviewer 3

One of the reviewers invited to review your manuscript has submitted the below review comments and the attached annotated PDF file. We believe these comments will help in improving your paper. Kindly address these comments in the revisions.

We have addressed and included where feasible the suggestions provided by the reviewer as we consider this would significantly further improve the paper.

#### Review Comments:

The study examines a set of ceramic sherds from central Nicaragua and the source materials for the production of the sherds. The authors have used standard methods (optical microscopy and p-XRF) to characterize their samples and performed multivariate statistical analysis (PCA) to carry out their provenance study. Although the manuscript contains some interesting data it has several important weaknesses which do not allow publication, because addressing these weaknesses go beyond a normal review process. In addition, some additional data would be necessary to substantiate the discussion of the manuscript. The main general points which need to be addressed are presented below.

Thank you for the questions raised. We substantially revised sections of the document and addressed the concerns provided to improve the paper and data presented.

1. p-XRF, the main method used in this study is semi-quantitative at best. In addition, it has not been presented explicitly. Although the authors used a series of standards to estimate accuracy, the texture of the sherds is different from that of the standards (solid ceramic sherds vs powder standards). In this sense the accuracy value shown is probably not applicable to the present study.

pXRF is used complementary to petrography and is a semi-quantitative technique which needs careful data interpretation and should indeed be systematically controlled. In order to matrix match the standards with the materials, pressed pellets were utilized for the calibration to facilitate reliable results within the capability of the technique. A multi-technique approach is therefore favorable, and in this manuscript, petrography was included as a robust technique to characterize the non-plastic (non-clay) fraction of the ceramics for provenance assessment. pXRF complements to incorporate the necessary overall chemical overview in order to draw meaningful conclusions.

2. The mineralogical analysis of the sherds and the source clays is elementary or totally missing. The description of minerals is mixed with that of rock fragments. The mineralogy of the matrices is not known. Also, the authors should have determined the mineralogy of the alleged source clays, which would substantiate their arguments for mixing source clays.

The mineralogy of clays changes upon firing and finally a sintered ceramic matrix is provided. Although mineralogical information of the mineral resources might be beneficial, it is not considered in this case to be a primary methodology to answer the research questions on ceramic production posed and is thus indeed only included in a limited capacity. Instead a multi-technique approach was set-up with petrography focusing on the non-plastic fraction to enable a comparison of the clay and ceramic and explain the contributions to the chemical composition.

Petrography is therefore crucial here as a robust and well-established technique and aids in explaining the chemical data. The minerals and rocks described all relate to the non-plastic fraction and not necessarily to the clay matrix itself (unless specified otherwise in these relatively low fired samples). Additionally, given the archaeological nature of the samples, a non-destructive chemical approach is seen as advantageous to incorporate the chemical aspect and to open up avenues for large scale analyses.

XRD would indeed provide mineralogical data on especially the raw clay material but would be considered rather restricted to further specify the petrographic and chemical groups and therefore not selected as a

primary analytical technique. However, the use of XRD for phase identification of raw materials would provide additional promising results to further characterise the clay raw materials.

We believe that in the text/table information related to difference size, quantity and type of mineralogical inclusions are presented sufficiently. These petrographic observations allow us to explain the chemical results as well as identify different clay preparations and recipes used from the potters, and to estimate from what type of geological environment minerals presented in the clay body originated. Mixing can be established on the basis of variable matrix optical activities as well as presence of temper, size and morphology of grains that might naturally be incompatible. We believe that the results of petrographic analysis presented in this study extensively cover the necessity that this methodology offers for interpreting chemicals results.

3. The authors have suggested firing temperatures based on the optical properties of the matrix of the sherds. These temperatures are highly speculative because they have not been substantiated with an independent test of evidence, such as neoformed high temperature phases. Finally, sherds with matrices which have different optical properties are proposed to indicate comparable firing temperatures, whereas the firing of sherds from Chontales D group has not been assigned to specific temperatures, although the matrix characteristics of these ceramic samples seem to be at least comparable to their counterparts from other groups.

We understand the questions raised here by Reviewer 3, however, XRD (which would be an option to characterize these phases) was not a priority to be performed here given these are technologically (low to medium fired) earthenwares. Therefore there is a limited chance that common high temperature phases such as spinel, cristobalite, mullite or Ca-silicates would be detected since temperatures in excess of at least 950°C are needed. The validation can be done by optical mineralogy/petrography which provide estimations, but with a resolution high enough to discern low, medium and high fired ceramics. This interpretation of the firing temperature is based on the extensive comparative literature on reconstructing ceramic technology through petrography (e.g. Patrick Quinn: Ceramic Petrography pp. 190-203). The temperatures provided are estimated on the observation of thermally induced change in the clay matrix. Quinn (pp.190-191) - *It is thought that the clay matrix of much traditional earthenware pottery loses its birefringence between 800-850 °C during firing. Therefore, samples with optically active clay matrices can safely be interpreted as having an approximate equivalent firing temperature of < 800-850 °C, and those with an inactive matrix in XP (crossing polarized light) are likely to have been fired > 800-850°C.* Sherds with similar optical properties are likely to have comparable firing temperatures.

Estimation regarding Chontales D has been added.

4. The quality of the results obtained from PCA is low because of the very small number of elements in their PCA. Also, with a few exceptions, in Figure 4 the source clays do not plot in the same areas as the sherds to support the idea of source clays.

We appreciate the critical evaluation of the data but we argue there is a consistent grouping available for determining source areas, as well as clays than can be excluded. While it is indeed correct that tracing individual clays might not be possible based on this information, clusters with common characteristics are clearly observable and can be distinguished with this analytical dataset, as also mapped out on the GIS map. Indeed, an extended or more high-resolution chemical technique might further elucidate this pattern, but that is beyond the scope of this current paper. Nevertheless, important elements or contributors in variability to assess a provenance for ceramics are represented, allowing for the PCA, of which the grouping is further confirmed by discriminant analysis. Other studies have yielded positive results to further develop the interpretative framework to estimate provenance



(Joshua J. Emmitt, Andrew J. McAlister, Rebecca S. Phillipps, Simon J. Holdaway, Sourcing without sources: Measuring ceramic variability with pXRF, *Journal of Archaeological Science: Reports*, Volume 17, 2018, Pages 422-432.)

5. The discussion is elementary, often unfocused, with errors of fact. The authors seem not to be aware of the speciation of Zr, Fe and Sr in certain minerals and key processes are described in an elementary manner. For instance, clay minerals do not “absorb” Fe-oxides. Also, the conclusions actually are a summary of the results rather than describing the most important findings of this work.

Clarifications are provided, and confusing sections amended. In the conclusions the most important finds and wider implications have been specified.

6. Several other

specific points have been marked directly on the annotated pdf file.

We thank the reviewer for the crucial suggestions. We addressed the points raised in the text and we amended the manuscript with regards to the comments listed. We consider that the text has been adequately improved after this review process.

## Highlights

- The first geochemical analysis of ceramics and clay samples is performed at the Mayales river subbasin, Central Nicaragua.
- Ceramics were produced locally from different clay outcrops, however, outliers from the Sulaco valley in the northeastern Honduras were spotted.
- A development in the sourcing of the raw material of ceramics by p-XRF.
- Spatial analysis in combination with geochemical analysis were performed and provided crucial information on the human-landscape interactions around Aguas Buenas.

# Geochemical and petrographic assessment of clay outcrops and archaeological ceramics from the pre-Hispanic site of Aguas Buenas (cal 400–1250 CE), central Nicaragua

Simone Casale<sup>\*1,2</sup>, Natalia Donner<sup>1</sup>, Dennis Braeckmans<sup>1,4,5,6</sup>, Alexander Geurds<sup>1,3,7</sup>

1 Faculty of Archaeology, Leiden University, Einsteinweg 2, 2333 CC Leiden, The Netherlands.

2 Royal Netherlands Institute of Southeast Asian and Caribbean Studies, Reuvensplaats 2, 2311 BE Leiden, The Netherlands

3 Institute of Archaeology, University of Oxford, 34-36 Beaumont St, Oxford, OX1 2PG, United Kingdom

4 Cranfield Forensic Institute, Cranfield University, Defence Academy of the United Kingdom, Shrivenham SN6 8LA, United Kingdom

5 Materials Science and Engineering, Delft University of Technology, Mekelweg 2, 2628 CD Delft, The Netherlands

6 Division of Geology, Earth and Environmental Sciences, KU Leuven, Celestijnenlaan 200E, 3001 Heverlee, Belgium

7 Department of Anthropology, University of Colorado-Boulder, 1350 Pleasant Street, Boulder, Colorado 80309, United States

**ABSTRACT:** This research characterizes and reconstructs clay procurement and production practices through the integration of in-situ portable XRF and petrographic analysis on ancient ceramics and clay materials recovered from the Mayales river subbasin (central Nicaragua). A particular choice for this study was the largest and arguably most significant archaeological site in the area, Aguas Buenas (cal 400–1250 CE), a pre-Hispanic indigenous agglomeration consisting of 371 human-made mounds of various shapes arranged in geometric patterns. Microanalytical approaches were applied to reconstruct the use of raw mineral resources in the production of ubiquitous pottery materials found at this site and in its immediate surroundings. The resulting compositional analysis produced geochemical and mineralogical data allowing for the characterisation of distinct, geologically-based compositional groups throughout the valley, improving on the limited geological data resolution previously available. The integrated microscopic and compositional analysis (through p-XRF) of archaeological pottery materials and raw clay samples, generates a number of hypotheses and insights about the nature of the Aguas Buenas site, and its role as a shared space among groups living in the Mayales river subbasin. Additionally, this study provides a solid research framework of investigation that can be employed for more detailed and extensive future studies on pre-Hispanic human occupation in this research area or elsewhere.

**Keywords:** Archaeological provenance, pre-Hispanic Nicaragua, Petrography, Ceramic microstructure, Geochemical analysis

\*Corresponding author.

Email address: [casale@kitlv.nl](mailto:casale@kitlv.nl) (S. Casale)

## 1. Introduction

This research aims to define ceramic provenance at a micro-regional scale through the application of both chemical and mineralogical techniques including the use of chemometric approaches. This data is crucial to characterise pre-Hispanic networks of clay procurement practices in the valley of Juigalpa within the Mayales river subbasin (Chontales region, central Nicaragua), with specific attention to the archaeological site of Aguas Buenas. Aguas Buenas is composed of 371 man-made mounds [1,2], making it the largest archaeological site with architectural remains of central Nicaragua, and the most extensive pre-Hispanic site documented in Nicaragua to date. The architectural features are geometrically arranged in an ellipsis that includes six concentric arcs, with a rectangular plaza in the center. Preliminary studies of the site evidence a long biography from 400 to 1200 CE and 1400 to 1600 CE, or the Cuisalá, Potrero and Cuapa phases in the original local chronology [3,4], which is currently under review. Recent detailed mapping and spatial analysis of the site proposed different moments for the construction of Aguas Buenas, which combines various construction preferences resulting in both circular and linear arrangements, alongside clustered structures [2]. The area around Aguas Buenas has been the subject of intensive surveying and excavations in recent years [5,6,7,8,9,10,11,12], in the process of which a total of 1671 surface structures were documented distributed across numerous clusters, and in combination with rock art panels [13]. These 1671 mounds are clustered in 47 different sites in the research area (Fig. 1).

The selected sample of pottery fragments reported here is derived from a large ceramic assemblage excavated from Mound 1 (M1) at Aguas Buenas, which provided macro-fabric, micro-chemical and petrographic variability in a particular “sealed” excavation context estimated to date between cal 400 and 800 CE, according to recent research at the site [14]. As these materials were used in the construction of the mound—both as filling and possibly also as offerings—, they represent choices made over a brief period of time, and therefore represent a suitable opportunity for assessing variability in the human use of clay and ceramic resources at the moment of construction of rows of individual mounds to form concentric arcs—one of the most defining geometric architectural features of the site. In addition, a pedestrian survey, conducted in 2015, aimed to identify clay sources offering reference materials critical to characterize the mineral resources present in the region [15], and the possibility to compare these with collected archaeological samples. Chemical analysis by means of portable X-ray fluorescence (p-XRF) combined with principal component analysis (PCA) showed clear chemical variability in clay outcrops, dividing the valley in main geochemical groups. In order to enhance initial results presented in Casale et al. [15] and characterise human clay procurement practices as well as technological manufacturing traditions at Aguas Buenas, mineralogical and textural analyses (thin section petrography) were performed, in combination with non-destructive chemical characterisation (by means of in-situ XRF analysis).

This research paper provides the first insights into pre-Hispanic ceramic production in central Nicaragua by integrating

data from a pedestrian surface clay survey with microanalytical information. The petrographic and compositional analyses are conducted on the pre-Hispanic ceramic assemblage excavated from M1 at Aguas Buenas, improving the resolution on technological practices at, and beyond, the site. This study improves the capability to establish the provenance of ceramics retrieved at Aguas Buenas, and has a wider impact on the archaeology of central Nicaragua as it provides an initial reference framework for ceramic provenance studies in this region.

## 1.1 Geological Context

The research area is located immediately east of the Central Nicaraguan Depression. The Nicaraguan Graben or Depression is the geologically youngest area of Nicaragua and is characterised by a mix of volcanic and sedimentary sequences of Paleocene-Eocene age. The volcanic rocks in this area are mainly composed of porphyritic basalt, basaltic andesite, and andesite to dacitic pumice [16,17]. The physiography of central Nicaragua includes elevations, plains, large inland lakes, their shores and its islands, as well as the hydrological drainage ultimately leading to the Caribbean Sea [18]. The topography of the Mayales river subbasin consists of isolated hills with a plateau shape and soft slopes that are characterised by sharp endpoints. Undulating mountains consist of more recent volcanic rocks, associated with the Tertiary-Quaternary, Coyol group (Late Miocene through the Late Pliocene, possibly up to the Pleistocene); while the eroded slope corresponds to the earlier Matagalpa group (Late Oligocene until Middle Miocene) [16,18]. Several large clay deposits have been formed on these geological substrates throughout the entire region. Most of these clay deposits are typically located in the vicinity of rivers and reasonably close to Late Holocene pre-Hispanic settlements, and therefore were likely used as a direct resource for the production of pottery [15].

## 2 Materials and methods

Macro-fabric analysis, thin section petrography and chemical characterisation were applied to a selected dataset of archaeological pottery fragments. The analysis of this study is associated with the results of Casale et al. [15] that presented results of p-XRF analysis on raw clay samples collected in the Mayales river subbasin (n=44 samples), and in the Zapatera island (n=5 samples), situated in the Nicaraguan Graben, near the western shore of Lake Cocibolca.

### 2.1 Sampling of clay and pottery fragments

The ceramic assemblage was obtained through a sampling strategy applied to the entire ceramic collection excavated from Mound M1 at Aguas Buenas. In total, 874 sherds were selected for macro-fabric examination, of which 65% consisted of large fragments (> 5 cm), while the remaining 35% were of smaller dimensions (< 5 cm). Most of the sherds were undecorated or featured a red or brown slip. The results of these macroscopic observations and the established

diversity of ceramic paste recipes provided the main rationale for sampling for compositional analysis (see [12]). The description of the sherds was based on five characteristics that are visible with a magnifying glass (10x) and an optical microscope: inclusions, fracture, hardness, compaction, and colour of the matrix. As a result of the macroscopic analysis, 49 archaeological pottery fragments were selected for petrography and, within this group, a subgroup of 30 samples was chosen for compositional analysis. The main goal of the chemical characterisation was to specifically test the possibility of linking the composition of the, (mostly) very coarse, ceramic pastes retrieved at Aguas Buenas, to the available collection of clays, and be able to use this as a baseline and initial reference for future provenance studies and hypothesis testing.

### 2.2.1 Chemical and petrographic analysis

Based on the provenance postulate, mineralogical and chemical composition of a homogeneous group of ceramics is closely connected to the mineralogical and chemical composition of different clay outcrops used in a production area [19]. Different analytical techniques such as neutron activation analysis (NAA), inductively coupled plasma mass spectrometry (ICP-MS), X-ray diffraction (XRD) and X-ray fluorescence (XRF) either as Energy Dispersive XRF (ED-XRF) or Wavelength Dispersive XRF (WD-XRF) provide precise compositional results of ceramics and clays and also relating to other archaeological materials such as obsidian, glass, metals and flints [20, 21, 22, 23, 24, 25]. However, with the exception of ED-XRF, which also exists in portable version (p-XRF), these techniques are destructive, requiring the extraction of a part of the sample. They are also time consuming and lab-based. As an alternative, p-XRF is non-destructive and expedient for use in the field. The major drawbacks, when compared with lab-based techniques, is that p-XRF has a lower precision to measure low-Z elements, due to the absence of a vacuum that is available for lab-based XRF. It also produces a lower energy X-rays, decreasing the range of elements that can be excited. For quantitative analysis, p-XRF technique has similar limitations to any other XRF devices with ideally the need of a smooth sample surface; a rather homogeneous specimen matrix; and calibration methods that are based on reference materials with matrix similar to the analysed material, allowing users to produce reliable data, in terms of accuracy, precision, and sensitivity. The portable and non-destructive nature of the instrumentation is a major advantage for further field studies with a suitable reference framework in place, however, data analysis needs to be carefully controlled and cautiously interpreted because p-XRF provides semi-quantitative data and it has been the scope of numerous research efforts to ensure reliable data [27, 28, 29, 30, 31, 32]. In this research, chemical analysis was carried out by p-XRF, which has been used as an explorative and especially non-destructive technique for provenance studies [27].

Prior to the analysis, samples were broken and, subsequently, the area of the fresh cut was polished and smoothed with

sandpaper to create a clean even surface. To optimize data reliability for each sample, three measurements in different areas were taken to compensate for possible heterogeneity. In general, the ceramics themselves do not show a macroscopically heterogeneous matrix, and occasionally visible larger grains were avoided. As it is shown in section 3.1, the texture of the selected samples is mostly medium coarse, and the average size of inclusions is < 0.5 mm. These characteristics increase the potential of testing for chemical identification of the assemblage, and to compare the results with petrographic observations.

The chemical analysis was conducted using a Bruker Tracer III-SD p-XRF device. The time of analysis was 120 seconds with 40kV and a 14  $\mu$ A. An Al-Ti-Cu filter was fitted to enhance the instrument's sensitivity in measuring mid-Z trace elements (Rb, Sr, Zr, Y, Nb), following the same methodology used by Casale et al. [15] to analyse the clay outcrops. Semi-quantitative results were obtained utilizing a custom empirical calibration for ceramic and soil materials. Quality control during analysis was monitored utilizing five rock and soil certified reference materials. These international standards are SRG-1 (Green River Shale), BIR-1 (Icelandic basalt), GSP-2 (Granodiorite Silver Plume), BCR-667 (Estuarine sediments), and CRM NIST-98b (Plastic clay). The following elements were obtained from the analysis: K, Fe, Ca, Ti, Cr, Nb, Ni, Sr, Rb, Y, Zn, and Zr. The elements Fe, Ca, Ti, Cr, Sr, Zr, **Rb** expressed a  $R^2 > 0.90$ , as an assessment of accuracy, and were considered for further bi-plots and statistical analysis. Precision—both repeatability and reproducibility—of the measurements was controlled at several instances by replicated analyses and was regularly assessed through the calculation of the relative standard deviation (RSD/%RSD) [33]. All selected elements generated %RSD values below 10% RSD. **A table with measured vs. certified values can be found in the supplementary material.**

In order to compare and interpret the chemical data of the ceramics, we created bivariate diagrams and additionally used a multivariate statistical approach as classification tools. The use of the multivariate statistical calculations allows for isolating and identifying chemical groups within the assemblage [34]. In particular, principal component analysis (PCA) was applied to compare clay raw materials with ceramics and assess possible provenances. **Discriminant analysis (DA) using Squared Mahalanobis distances was further used to test the groups created as a result of the petrographic observations and compositional analysis.** PCA is additionally a powerful tool to identify which elements contribute to the final composition of the sample. This technique allows for reducing the multivariable dataset to two dimensions, and they are frequently employed to identify subgroups as well as to verify groups created through petrography, stylistic features, or other approaches [35].

For optical mineralogy, thin sections of ceramic fragments were prepared and their structure and composition were observed with a polarizing microscope (Leica DM750P), which uses transmitted plane-polarized (PPL) or cross-polarized (XP) light. The petrographic analysis aimed to characterise the two most important components that constitute a ceramic

material: the clay matrix and the non-plastic inclusions. Moreover, it is possible to observe the characteristics of voids, pores, and the presence of slip or paint layers, as well as other types of surface treatment applied by potters [36]. The interpretation of these features in comparison with the geological context of the archaeological site from where the materials were excavated, allows us to formulate hypotheses both about provenance, as well as to discriminate materials formed from different mineral resources [37,38]. Furthermore, thin section analysis provides information on the employed technological procedures involved in the manufacturing of pottery [37]. For instance, through the observation of the birefringence of the clay matrix, it is possible to estimate the firing temperature at which the earthenware was fired. The firing process causes the sintering of the clay components and mineral/rock inclusions, with a loss of ‘optical activity’ of the matrix. Higher temperature induces important structural changes and the matrix becomes anisotropic, with inclusions that melt and vitrify, creating a more glassy aspect. On average, a clay matrix loses “optical activity” between 800–850 °C. Thus, samples that yield an optical clay matrix are considered to have been fired at temperatures of < 800–850 °C, while those having an inactive matrix are usually fired at temperature > 800–850 °C [37]. Photomicrographs were taken with a factory-built Leica camera at the Faculty of Archaeology at Leiden University.

### 3 Results

#### 3.1 Macroscopic analysis

The assemblage examined included sherds representing different parts of vessels, such as bodies, necks, and rims. Analysis of technological macro traces showed a fashioning technique without the application of rotary kinetic energy, on assembled elements—coils—implying gestures of digital and hand pressure through pinching, drawing, and slight crushing. No percussion was identified, aside from some traces of discontinuous palmar beating. In particular, coils were majorly equidistant, placed alternatively from inside to outside and vice versa. Fashioning was highly homogenous within the entire sample and within the various parts of the vessels, with small variances in coil size, which ranged from 1 to 2 cm. Pre-forming techniques featured a higher variability than in fashioning, with both leather hard (shaving) and wet clay techniques (scraping). For finishing, the microtopography showed horizontal striations linked to brushing and/or smoothing techniques on both wet and leather hard clay. The most commonly applied surface treatment was burnishing; decoration mainly consisted of slips and paint, with a wide range of colors but mostly red, black, red on orange, red on orange on white, red on white, and brown on orange. The high degree of erosion found, together with post-depositional layer attached to the sherd walls and the low firing temperature in some sherds, made macro-trace analysis extremely challenging.

The macroscopic analysis of pastes revealed that inclusions found in the ceramic pastes were coarse, measuring



approximately 0.5–1 mm, and their colours varying from white, red, and brown to black. 2% of the sherd assemblage has a highly fine grain matrix (< 0.1 mm), which can be considered as an outlier cluster. In general, the main differences were in hardness and colour. Variability in the core-margin relationship, cross-section and surface Munsell colors suggests that firing practices involved different temperatures, duration of firing, and position of the vessel (or vessel part) in relation to the fuel source—possibly an open hearth firing context. There may have been an intentional change from oxidizing to reducing firing conditions, based on the current observations. Nevertheless, partially oxidizing firing atmospheres were observed frequently, as identified by a characteristic “sandwich” colouring in the matrix [39].

A total of 24 homogenous macroscopic clusters were identified, featuring clay recipes that mainly contain feldspars, dark mica, rock fragments, and quartz. These sets of inclusions were repeated in different sizes and frequencies, resulting in a homogenous assemblage comprised of several groups. The orientation of the inclusions was subparallel, concentric, and oblique, and chaotic, which is consistent with the coiling technique for pre-forming vessels [37]. Voids were generally of plate-like, oval-sphere, and irregular shapes, and their orientation was also subparallel, concentric, oblique, and chaotic. These macro-groups defined according to their paste characteristics were then used in the secondary sample selection for thin section and compositional analysis.

### 3.2 Petrographic analysis

A total of 49 sherds was selected for petrographic analysis and subdivided into six petro-groups. A detailed overview of the six petrographic groups identified, and their characteristics, is provided (Table 1, and Figures 2 and 3). Most of the inclusions are connected to a relatively homogeneous mineral composition derived from a basic intermediate igneous parent rock, and in some cases, there are samples with a more mafic (AB-N-45, AB-L-68, AB-D-45) or more andesitic (AB-H-68 and AB-S-78) composition. The ceramic assemblage does not show evidence of calcareous rock inclusions visible through the optical microscope, however, calcareous microscopic inclusions might be present in the matrix as is pointed out by the chemical analysis (see below). The most common inclusions that can be related to these mafic/intermediate rocks are plagioclase, basalt, andesite, pyroxene, olivine, and rarely biotite, as well as hornblende grains. The mineralogy of the inclusions present in the ceramic body is consistent with the geology of the area, which is mainly characterised by Oligocene and mid-Miocene rocks [16].

From a technological perspective, the interpretation of the size, shape and distribution of the inclusions within the matrix suggests that the majority of ceramics were probably not tempered by the intentional grinding of rocks. However, adding temper by re-using ceramic materials (i.e. grog) was an identified practice. Moreover, the matrices of the sherds show evidence of possible mixing of different clays, with at least two clearly distinguishable pastes noted in the same fabric

(Fig. 2, caption 11). In particular, it seems that a lighter, more calcareous **fine clay matrix** might occasionally have been added to, as indicated, for instance, by samples AB-C-74, AB-A-71X, AB-M-68X, and AB-D-29, **however, there is no evidence of medium-coarse rock inclusions of calcareous origin.**

The mineralogical characterisation of the samples, examined through thin section petrography, yielded four main compositional clusters (Chontales A, B, C and D). Both petrofabrics C and D have been subdivided to incorporate systematic variations with the respective groups. In total six petrofabrics have been characterized and described.

#### *Chontales A*

This fabric is characterised by an orange-brown optically active matrix with an estimated firing temperature **lower than 800–850 °C [37]**. The edges of the samples feature traces of a post-depositional calcite layer and, in a few cases, also a red line below this surface, which may be a trace of finishing and/or surface treatment techniques. The aplastic inclusions show significant variations in dimension. Monocrystalline subangular to subrounded quartz and plagioclase (euhedral and non-euhedral) are the most common inclusions (150–500 µm). There are also medium-coarse sized inclusions (150–600 µm) of chert, granite, basalt and andesite, which vary between subangular and subrounded shapes. The other, much more rare, aplastic inclusions are olivine, orthopyroxene, clinopyroxene, and biotite. The grain size is up to 600 µm, and in a few cases, there are coarse subrounded inclusions of clay pellets and rare grog particles of up to 2000 µm.

#### *Chontales B*

Fabric B is characterised by a dark reddish brown optically inactive matrix, suggesting a firing temperature above 850 °C. The non-plastic inclusions are well-sorted and characterised by a bimodal distribution of fine grains with one range of 150–250 µm and a second range of < 150 µm. Monocrystalline plagioclase and quartz are the most common inclusions. They are characterised by subangular and subrounded shapes. There is a limited number of rock inclusions such as granite, basalt, and chert. Andesite is very rare in these samples. The size of rock inclusions ranges from 150 to 250 µm, with a few isolated inclusions exceeding 500 µm. The other aplastic inclusions are opaque minerals, orthopyroxene, clinopyroxene (augite), and olivine. Their quantity is much lower (< 5%) in comparison to quartz and plagioclase, which comprise 70% of the total inclusions. As with Chontales A, there is a low number of clay pellets and very coarse grog (1000–2000 µm).

#### *Chontales C*

Petrographic Fabric C can be defined as the major group in the study. It contains, however, systematic variations that yielded a further subdivision of the ceramics attributed to this petrographic group.

#### *Chontales C-1*

This fabric is composed of a non-calcareous orange-yellowish brown slightly optically active matrix, suggesting a firing

temperature lower than 800–850 °C. The outer surface shows traces of a post-depositional layer of calcite. The aplastic inclusions are tri-modal, ranging from 150 to 600 µm. This is a significant size variation, which could be interpreted as an absent or poorly executed sorting strategy. The most common mineral inclusions are quartz, feldspars (k-feldspar and plagioclase crystals) and chert with angular, subangular, subrounded and rounded shapes. There are also minerals of volcanic origin such as orthopyroxene, clinopyroxene (either augite or diopside), olivine, and a very low quantity of large crystals of biotite and hornblende. The rock inclusions are composed of granite and andesite. Basalt occurs in minor quantities and dimensions. A main discriminator is the presence of clay pellets and grog in smaller dimensions (300 and 400 µm) when compared to fabrics A and B.

#### *Chontales C-2*

This subgroup consists of a more darkish brown to greyish-brown non-calcareous matrix. The matrix ranges from optically active to inactive, suggesting different firing temperatures from 600 to 800 °C. Once again, a post-depositional calcite layer covers the surface of the samples a characteristic shared with groups A and C-1. Non-plastic inclusions vary in size, ranging between 150 and 600 µm. Quartz and plagioclase are the main inclusions, followed by granite. There are large coarse inclusions of chert in variable shapes, from subangular to rounded. The other rock inclusions present are basalt and andesite, and these vary from fine to coarse (150–650 µm). Less frequent aplastic inclusions are orthopyroxene and clinopyroxene (augite and rarer diopside), opaque minerals, olivine and (very rare) hornblende and biotite. There are a few isolated cases of large clay pellets (up to 1300 µm), with the average size range being between 300 and 400 µm. The group does not present grog grains.

#### *Chontales D*

A further group of samples that shares both technological, matrix and mineralogical features but also exhibit a few differences is group D. Therefore, a subdivision in Group D-1 and D-2 can be defined where D-2 is considered to be the result of mixing multiple raw clay sources, based on the presence of mixing lines in samples (Fig. 2, caption 11), with one of these sources being highly similar as that of the source of Group D-1. The optical activity of the ceramic matrix of these two groups suggests that the vessels were fired at a relatively low temperature < 800–850 °C.

#### *Chontales D-1*

Group D-1 has a light orange-brown optically active matrix. Similar to Groups A, C-1, and C-2, traces of post-depositional calcite were observed on the surface of the sherds. The fabric is characterised by a non-calcareous trimodal matrix, which includes very coarse (1000–2000 µm), coarse (500–1000 µm), and medium (250–500 µm) inclusions. The largest aplastic inclusions are chert (300–1000 µm), granite (200–800 µm), andesite (250–650 µm), and k-feldspars (150–600 µm). The

basalt inclusions are smaller (250–300 µm), and either rich or poor in iron content. Quartz and plagioclase are the most common inclusions, and are mostly subangular and subrounded in form. Other inclusions are characterised by single crystals of opaque minerals, orthopyroxene and rare augite (300–150 µm) as well as olivine (150–50 µm), while hornblende and biotite are very rare. The main distinguishing feature, besides the large rock inclusions, is the presence of large grog grains distributed in the matrix (400–1400 µm).

#### *Chontales D-2*

The fabric is characterised by a light yellowish-brown matrix, which can be identified as a little more calcareous when compared to groups A, B and C. The distribution of the inclusions is trimodal, characterised by medium and coarse inclusions, which range from 250 to 1000 µm and some very coarse grains measuring between 1200 and 1600 µm. There is a high abundance of coarse chert grains (300–1200 µm) of subangular and subrounded shapes. The other rock inclusions are granite, basalt and andesite from a subangular to subrounded form, which are marked by a significant variation in size (200–1000 µm), suggesting a natural presence of these rocks in the raw sources rather than the addition of temper. Quartz and K-feldspars are the most common inclusions and have a significant variation in dimensions. The quartz pieces vary between 100 and 650 µm and are mostly angular to subangular. The K-feldspars have dimensions between 500 and 1500 µm, while plagioclase, being the most abundant type, measures 150 µm on average. Sanidine is present in minor quantities with dimensions between 700 and 1000 µm. The other inclusions that are present in minor quantities are opaque minerals, orthopyroxene, augite, biotite, and olivine. As in groups A and B, and D-1, grog fragments are also present and vary in dimension (400–500 and 1100–1600 µm). In contrast to groups A and B, clay pellets of very coarse size were not identified.

### **3.3. Chemical analysis**

The results of the chemical analysis for the 30 sherds are integrated with the petrographic grouping highlighted in the previous paragraph and shown in Table 2 and table 3. The scatterplot that compares CaO and Zr (Fig. 3) displays how the values in Zr tend to be heterogeneous throughout the dataset, while there is a correlation between the values of Sr and CaO, which can be associated with the carbonate component of the clays. In contrast, Zr accumulates particularly in coarse and heavy inclusions as a result of high-energy environments, such as river sedimentations [40]. As illustrated in the charts (Fig. 3), the petrographic groups are not unequivocally reflected in the chemical composition through these single element observations. In particular, Chontales A (AB-G-71, AB-A-60, AB-P-71, AB-S-78) is characterised by a high correlation in Sr and CaO and a low correlation in Zr (Fig. 3). Samples AB-G-71 and AB-P-71 were also grouped together in the petrographic analysis. The values of Sr and CaO can be associated with the presence of feldspars such as

k-feldspar and plagioclase, or their weathering products [41] since the carbonate content was exceedingly low in this type of ceramics. These two samples also contain low presence of basalt inclusions. Cr can generate issues in the analysis with p-XRF [30], and it was not included in further statistical calculation (see further in the discussion). Chontales B has a composition that can be connected to Chontales A, and only the Cr values are around the detection limit of the p-XRF. Samples belonging to group Chontales C-1 show lower values in Sr and CaO, which can be related to high levels of sediment weathering, the mobility of these elements, or rather, the presence of plagioclase, as well as carbonates. The high values in Fe are confirmed by the presence of orthopyroxene, basalt and iron-rich inclusions in samples AB-N-45, AB-L-78, and AB-L-68. These three samples were already grouped together in the petrographic analysis. A similar composition is also shown by the sherds in group Chontales D-1, which are characterised by a high correlation of Fe, Ti, and Ca. The first two elements are related to the presence of pyroxene minerals while calcium is associated with the plagioclase. Groups Chontales C-1 and C-2, in contrast to the previous groups (D-1 and D-2), are enriched in Sr. The lower value in Fe for samples AB-T-60 and AB-T-83Q can be linked to presence of granite and the low number of rock inclusions (e.g. andesite) and the total absence of basalt in contrast with other ceramic samples. For sample AB-E-68X, this low value can be connected to the matrix, which is characterised by a yellowish colour and considered an iron poor clay.

#### 4 Discussion

The correlation of the petrographic groups with the compositional analysis through the observation of single element values and element ratios was not unequivocal in attributing discrete sources. It is important to highlight that when such coarse grain ceramics are analysed together with the temper added during the manufacturing process, as in this case study, nonplastic inclusions may have a critical impact on the chemical composition results. The coarse grain size can obscure the presence of other minerals or the composition of the clay matrix which *in extremis* could influence the compositional results. It is thus essential that any potential problem is taken into account in discussing the p-XRF results. Multiple readings on each of the samples were collected in order to mitigate part of this potential variation, as the aim of the analysis is to delineate systematic differentiations within the ceramic assemblage.

The results of the clay survey of Casale et al. [15] demonstrate how the majority of the suitable clay outcrops are located near the banks of rivers, as a result of fluvial sedimentation. It is likely that differential fluvial and alluvial depositional processes throughout the valley, which vary from seasonal streams to perennial rivers (such as the Mayales river), may have had an impact on, for example, the accumulation of Zr and by extent heavy minerals (such as zircon) [40]. This results in a variable elemental composition within the raw materials employed for the preparation of the pottery. The

scatter-plot of Ca and Sr (Fig. 3) shows that the two elements are partly correlated as expected, suggesting that the presence of Sr in the ceramics can be associated to both a microcrystalline (carbonate) composition of the raw materials, but more significantly relates to the feldspar component (and particularly plagioclase) of the fabric groups [40].

In order to successfully compare and integrate the analytical results of both clay and ceramic materials, we applied a multivariate statistical methodology for group assessment and variability. PCA and DA were calculated in SPSS using  $\text{Fe}_2\text{O}_3$ , CaO,  $\text{TiO}_2$ , Sr, Zr and Rb. Cr and Nb were not included to not mislead the interpretation of the calculation. The first has a high variability through the assemblage while the latter is present in very low quantity (on average < 5 ppm). DA were determined to assess the validity of the ceramic groups created through the petrographic observations. Results demonstrated that 79.2% of the specimens were grouped correctly as with the petrography. Group C-1 has one sample (AB-G-71) that was assigned to C-2 and C-2 has one sample (AB-A-60) assigned to C-1. The same occurred with D-1 and D-2, where AB-A-71Y was assigned to D-2 and AB-H-68 was connected to D-1. Overall, the DA gave a positive result demonstrating that only five samples out of 30 were re-grouped differently, and four of that, were re-grouped between subgroups of the same main groups. Geochemical similarities are expected between subgroups of the same petrographic groups, due to the presence of similar mineral inclusions.

A PCA bivariate biplot was calculated including all samples, both reference clay data ( $n = 44$ ) from Casale et al. [15] and representative sherds ( $n = 30$ ), in order to understand possible connections between the regionally available clay raw materials and ceramics from Aguas Buenas. An important result of the statistical calculation is that, in contrast with the two-elements plots, when more significant elements are analysed ( $\text{Fe}_2\text{O}_3$ , CaO,  $\text{TiO}_2$ , Sr, Zr, Rb), the petrographic groups identified show a consistent internal geochemical composition. Table 4 shows the results of the compositional analysis for the clay samples, the results of the grouping made by Casale et al. [15], and the ceramics linked to the possible clay sources, following chemometric approach through PCA. Figure 4 graphically illustrates the comparison through PCA, in which both soil and ceramic samples are shown according to their compositional groups for clays and petrography for ceramics. The majority of the ceramic samples cluster together parallel to petrographic grouping but diverging from some of the clay outcrops analysed. Overall, petrographic and chemical data of the ceramics provides consistent observations and confirm the presence of different resource areas. In order to further test the reliability of the groups identified in PCA, Squared Mahalanobis distances were calculated to assess predicted and statistically assigned groups. Results indicated that 75% of the ceramics and clays were assigned to the same clusters as those evidenced in PCA. Generally, some overlap exists between Chontales A, D-1 and D-2 arguing for chemically related clay outcrops which can however be clearly separated through optical microscopy. Chontales B is clearly discerned from the rest of the ceramics, both mineralogically as well as chemically. Chontales C1 and C2 on the other hand overlap more significantly and can be considered chemically

consistent which suggests the difference between C-1 and C-2 would be rather production related.

A positive attribution can be made for six clays outcrops (D12.1, E5.1, M3.2, M3.1, C12.1 and N4.1) which cluster with 13 ceramics in three major groups. These results propose that some of the ceramics retrieved in Aguas Buenas were likely produced with local clay readily available in the surrounding environment. The outcrop M3.2 matched seven ceramics from Chontales A (AB-E-68X, AB-O-74, AB-I-83), Chontales D-1 (AB-A-20, AB-A-71Y) and Chontales D-2 (AB-B-75, AB-L-68), while N4.2 and M3.1 clustered with Chontales C-2 (AB-N-60), Chontales D-1 (AB-M-83). The clays samples D12.1 and C12.1 matched with AB-G-71 and AB-A-60 from petrographic groups Chontales C-1 and C-2.

Generally, both ceramics and clays yielded low-calcareous crystalline matrices associated with basalt and andesite parent rocks. Figure 4 shows the resulting geographic distribution of clay samples that were associated with Aguas Buenas' ceramics, together with the location of the other mounds in the valley, and the locations that yielded surface ceramic materials. Table 4 lists these associations of the ceramic samples with the corresponding mineral resources. Regarding the mineral resources, Group 1 (G1) includes only the (clay) samples from the Zapatera Island, yielding systematic higher values of  $\text{TiO}_2$ , Cr, and  $\text{Fe}_2\text{O}_3$ , in contrast to the other groups. DA considers this group independent from the rest of the assemblage with 100% of correctness. The Zapatera Island is a shield volcano, which is characterized by basaltic/andesitic rocks and the  $\text{Fe}_2\text{O}_3$  contents can be connected to mafic minerals such as pyroxenes, biotite and olivine which characterized the landscape. These clay samples cluster outside any other groups, suggesting these can be positively discriminated and thus that the ceramics recovered at Aguas Buenas were not manufactured with clays from the island.

Different technological practices are identified as well. Chontales B, for instance, has the finest matrix in the assemblage. The fine size of the inclusions can be the result of sieving practices that eliminated coarse grains affecting the final geochemical composition and workability of the matrix, which strongly diverge from the rest of the assemblage. Recent observations have connected these finds as part of the Sulaco valley technical complex in northeastern Honduras (R. A. Joyce, personal communication, October 2019), which would further explain not only the wide difference in petrographic and geochemical values, but also in aesthetic perceptions. Petrographic groups Chontales C (C-1 and C-2) as well as Chontales D (D-1 and D-2) show a similar internal chemical composition as demonstrated by PCA and DA, supporting the petrographic observations.

Looking at the extension of the clay outcrops, the clay deposits that yielded the highest similarity with the archaeological ceramics (M3.2, M3.1, D12.1, C12.1, N4.2, E5.1) are also the largest in extension [12, 15]. It is indeed likely that populations in pre-Hispanic times quarried those sources, although a more precise identification of specific outcrops along this river system, or its tributary streams and creeks, is currently not possible.

Furthermore, the combination of data regarding clay outcrops location and specific archaeological site location in the



valley provides interesting data that clarify on human-landscape interaction and mobility. Each clay outcrop has archaeological sites in the vicinity, often within less than 2 km (Fig. 4). However, these sites were not contemporaneous to Aguas Buenas, dating to a later period [14]. This enables further studies on the ceramic materials retrieved from these sites, and to understand possible connections with Aguas Buenas.

Consequently, the differences in sizes between documented exposed clay areas seem to be relevant in clay procurement choices. If we consider a long-term use of these natural resources, then it is possible that inhabitants of the area looked for the largest and perhaps the most sustainable sources available, in order not to rapidly exhaust them [42]. Large quarries were not employed for massive production, since we have no evidence for such manufacturing practices in the history of the subbasin. Therefore, we can also propose that the selection of larger deposits ensured the continuity of socially learnt clay procurement practices over time. Such use strategies were likely shared among different communities of practitioners.

The optical microscopy analysis outlines the presence of different paste groups and, in some cases, the technological choice of mixing more than one clay for producing vessels. Clay mixing can be due to several reasons, from simple habit to liquidating older supplies [43], but mixing can also aid in achieving specific desired features such as plasticity, firing resistance and/or dimension of the pots [42, 44, 45, 46]. In order to control these features, potters can mix different clay sources for improved results. The compositional and petrographic analyses show that there are some pots consistently made with more fine grains (such as AB-T-78A, AB-T-60, AB-T-83Q), and others with coarser grains (for instance Chontales D-1 and D-2).

Clay outcrop M3.1 is the closer one to Aguas Buenas (< 3 km), has the largest surface area (100 x 100 m), and also matches other samples, although to a lesser extent. Outcrop N4.2 is located at less than 1 km distance from outcrop M3.1 and approximately 5 km from Aguas Buenas, suggesting the possibility of mixing more clays to reach a better workability of the paste, as was highlighted by the petrographic observation specifically for groups Chontales D-1 and Chontales D-2. Therefore, clays from M3.1 and N4.2 may have been employed by the population and strategically mixed with other clays, or tempered, reflecting different technological choices and production practices.

## Conclusions

Since 2009, the detailed archaeological investigation of the Aguas Buenas monumental site by the *Proyecto Arqueológico Centro de Nicaragua* (directed by Geurds), and its relatively unique form and dimensions, has opened a range of questions concerning the sites' construction, associated practices and wider importance in the Mayales subbasin. As part of this corpus of studies, we have here analysed practices related to clay procurement and pottery-making, using mineralogical



827  
828  
829 and geochemical methods. The integration of both optical microscopy with non-destructive XRF analysis provided the  
830  
831 necessary basis for building an interpretative framework for provenance. The petrographic analysis demonstrates that,  
832  
833 even when excavating a single mound (M1) and within a similar volcanic geological substrate, sherds show considerable  
834  
835 mineralogical differences, leading to clear divisions into different provenance groups. The further use of the p-XRF as a  
836  
837 connected chemical field method, confirmed the presence of systematic compositional groups. Results are promising and  
838  
839 suggest the existence of ceramic materials that were manufactured with raw clays from diverse local origins as well as  
840  
841 materials produced with clays from outside the Rio Mayales subbasin. The statistical analysis indicates that six clay  
842  
843 outcrops, compositionally matching the ceramics from Mound M1 at Aguas Buenas, are located near other clusters of  
844  
845 mounds, zones of high-intensity surface ceramics, but mostly with larger clay deposits also being available nearby. In  
846  
847 particular, the results show that, even though there are suitable clay outcrops within a 1 km radius of the site [15], raw  
848  
849 materials are chosen from outcrops between 3 and 5 km away. This is relevant when considering the people that built  
850  
851 Aguas Buenas, and their relationship to the surrounding landscape. The exploitation of several raw material sources  
852  
853 simultaneously, for example, implies a detailed knowledge of the territory, as well as pointing to several different groups  
854  
855 engaged with pottery-making activities.

856  
857 The methodological framework entailed a combination of petrographic and compositional analysis of ceramic materials  
858  
859 and clay samples, generating information to support a number of conclusions about the nature of the pre-Hispanic Aguas  
860  
861 Buenas site and its role among people living throughout the Mayales river subbasin. Also, it shows variability in pottery  
862  
863 production operational sequences, from clay procurement –andesitic vs. basaltic clays–, clay preparation–tempering,  
864  
865 mixing, and sieving practices–to surface treatment–smoothing and slipping gestures.

866  
867 It is likely that additional systematic and large-scale archaeometric analysis based on, for example, more high resolution  
868  
869 compositional techniques (such as for example XRD, INAA, and ICP-MS), applied to cultural materials from sites  
870  
871 spanning the entire subbasin, will further clarify the extent of connectivity between groups in central Nicaragua. XRD  
872  
873 analysis, for instance, allows to characterize the presence of different clays in the same ceramic body, clarifying further  
874  
875 on the technology and clay preparation strategies. Ultimately, this research provides a first framework of investigation  
876  
877 that can be employed in future extensive studies on the Mayales river subbasin, and the chosen methodology holds  
878  
879 potential for its application in other regions as well.

## 880 881 Acknowledgments

882  
883 We would like to thank Kaz van Dijk, Gabriel van der Pluijm, and Pol Miguel Salles for their invaluable assistance during  
884  
885 fieldwork. Also, we are indebted to Leontien Talboom, who assisted in the survey, and built the database that was used

in the laboratory. We gratefully acknowledge the aid of Alejandro Arteaga Saucedo, who provided relevant data that made the design of the maps possible. We express our gratitude to the Nicaraguan Institute of Culture, and in particular its co-director Luis Morales Alonso and the director of the Archaeology Directorate, Ivonne del Carmen Miranda Tapia, for their continued support of the project, and for issuing the permits to export samples. The Archaeological Museum Gregorio Aguilar Barea in Juigalpa was very supportive in the early stages leading up to this research. We are also indebted to Loe Jacobs and Eric Mulder for their enthusiasm and relentless help at the Laboratory for Artefact Studies at the Faculty of Archaeology, Leiden University. Finally, the clay survey was greatly facilitated by Eleuterio Castillo, our local guide and friend, whose key knowledge of the landscape and the communities proved vital. Finally, we would like to thank the three anonymous reviewers for their constructive suggestions to improve this paper.

**Funding:** This research was made possible by the Netherlands Organisation for Scientific Research (NWO) VIDI grant “Networked practices of contact: Cultural identity at the Late prehistoric settlement of Aguas Buenas, Nicaragua, AD 500–1522” (PI Alexander Geurds).

## References

- [1] Geurds, A., Donner, N. R., Arteaga, A., Angeles, R., Torreggiani, I., Donner, D., Ayala L., A., Mendoza C., L., Murguía L., J. (2015). Reporte Preliminar Proyecto Arqueológico Centro de Nicaragua (PACEN) Novena etapa. Unpublished report, INC, Managua.
- [2] Auzina, D. (2018). Monumentality by Communities. Mapping the Spatial Logic of the Pre-Hispanic Site Aguas Buenas (AD 400-1600) in Central Nicaragua. Research Master thesis, Leiden University.
- [3] Gorin, F. (1990). Archéologie de Chontales, Nicaragua (3 vols.). Dissertation, Université de Paris I, Paris.
- [4] Rigat, D. (1992). Préhistoire au Nicaragua: Région Juigalpa Vol 3. Dissertation, University of Paris.
- [5] Geurds, A. (2010). Proyecto Arqueológico Centro de Nicaragua. Temporadas 2010-11 El Ayote-RAAS. Unpublished report, INC, Managua.
- [6] Geurds, A. (2012). Proyecto arqueológico Centro de Nicaragua. Temporada 2012. Informe Técnico Final. Unpublished report, INC, Managua.
- [7] Geurds, A. (2013). Proyecto Arqueológico Centro de Nicaragua. Temporada mayo-junio, 2013. Informe. Unpublished report, INC, Managua.
- [8] Geurds, A. (2014). Proyecto Arqueológico Centro de Nicaragua (PACEN). Séptima etapa: prospección intensiva, mapeo total y excavación en sitio Aguas Buenas (cuarta temporada), comarca San Isidro, Juigalpa, Chontales. Unpublished report, INC, Managua.
- [9] Geurds, A., Terpstra, D. (2017). Circular Reasoning in Mound Building? Large- scale Planned Construction Patterns at the Aguas Buenas Site (A.D. 400–1525). In: War & Peace: Conflict and Resolution in Archaeology (pp. 47–59). Proceedings of the 45th Annual Chacmool Archaeology Conference, edited by Adam K. Benfer. Chacmool Archaeology Association, University of Calgary, Calgary, Alberta, CA.
- [10] Vlaskamp R. J. C., Geurds A., Jansen R. (2014). Reporte de las investigaciones arqueológicas entre 2011–2014 en el sitio prehispánico de Aguas Buenas, Chontales, Nicaragua. *Mi Museo y Vos* 8(29), 6–12.
- [11] Arteaga S., A. (2017). Reconstrucción del paisaje social prehispánico en la microcuenca del río Mayales, Chontales, Nicaragua. Unpublished Master thesis, Universidad Nacional Autónoma de México.
- [12] Casale, S. (2017). Pre-hispanic clay roads. Evaluation and interpretation of ceramic products and raw clay procurement in the Rio Mayales Subbasin, Chontales, Nicaragua. Research Master thesis, Leiden University.
- [13] Donner N. R., Arteaga A., Geurds A. & Dijk K. van (2018). Caracterización inicial de los sitios arqueológicos en la subcuenca del río Mayales, Departamento de Chontales, Nicaragua. *Cuadernos de Antropología* 28(1): 1–26
- [14] Donner, N. R., Geurds, A. (2018). The valley of Juigalpa, Mayales River Sub-basin Microregion (Chontales, Nicaragua) Date list I. *Radiocarbon* 60(2), 1-10.

- [15] Casale, S., Donner, N. R., Braekmans, D., Geurds, A. (in press). Pre-Hispanic and contemporary raw materials use in earthenware production in the Río Mayales subbasin, Chontales, central Nicaragua. In Klinkenberg, V., R. van Oosten and C. van Driel-Murray (eds.). *A Human Environment. Studies in honour of 20 years Analecta editorship by Prof. Dr. Corrie Bakels. Analecta Praehistorica Leidensia (APL) 50*. Leiden: Sidestone Press. ISBN 978-90-8890-906-1
- [16] Arengi, J. T., Hodgson, G. V. (2000). Overview of the Geology and Mineral Industry of Nicaragua. *International Geology Review*, 42(1), 45-63.
- [17] Hradecký, P. (2011). Introduction to the special volume "Subduction-related igneous activity in Central America – Its nature, causes and consequences". *Journal of Geosciences* 56 (1): 1-7.
- [18] Garayar, J. (1972). *Geología y depósitos de minerales de la región de Chontales y Boaco. Catastro y Reservas Minerales, División de Geología, Informe, (11), Managua*.
- [19] Weigand P. C., Harbottle G., Sayre, E. V. (1977). Turquoise sources and source analysis: Mesoamerica and the Southwestern USA. In: Earle T. K. and Ericson J. E. (eds.), *Exchange Systems in Prehistory* (pp. 15–34). New York: Academic Press.
- [20] Glascock, M. D., Neff, H., Stryker, K. S., Johnson, T. N. (1994). Sourcing archaeological obsidian by an abbreviated NAA procedure. *J. Radioanal. Nucl. Chem.*, 180 (1), 29–35.
- [21] Gratuze, B., 1999. Obsidian characterization by laser ablation ICP-MS and its application to prehistoric trade in the Mediterranean and the Near East: sources and distribution of obsidian within the Aegean and Anatolia. *J. Archaeol. Sci.* 26 (8), 869–881.
- [22] Sharrat, N., Golitko, M., Williams, P.R., Dussubieux, L. (2009). Ceramic Production during the Middle Horizon: Wari and Tiwanaku Clay Procurement in the Moquegua Valley, Peru. *Geoarchaeology* 24(6), 792-820.
- [23] Finlay, A., McComish, J., Ottley, C., Bates, C., Selby, D. (2012). Trace element fingerprinting of ceramic building material from Carpow and York Roman fortresses manufactured by the VI Legion. *Journal of Archaeological Science*, 39 (7), 2385-2391
- [24] Guerra, M.F., 1998. Analysis of archaeological metals. The place of XRF and PIXE in the determination of technology and provenance. *X-Ray Spectrometry* 27, 73-80.
- [25] Hughes, R.E., Högberg, A., Olausson, D. 2010. Sourcing flint from Sweden and Denmark: a pilot study employing non-destructive energy dispersive X-ray fluorescence spectrometry. *Journal of Nordic Archaeological Science* 17, 15-25.
- [26] Speakman, R.J., Little, N.C., Creel, D., Miller, M. R., Iñáñez, J. G. 2011. Sourcing ceramics with portable XRF spectrometers? A comparison with INAA using Mimbres pottery from the American Southwest, *Journal of Archaeological Science* 38 (12), pp. 3483-3496.
- [27] Shugar, A., Mass, L. (2012). *Handheld XRF for Art and Archaeology. Vol. 3*. Leuven: Leuven University Press.
- [28] Morgenstein, M., Redmount, C. A. (2005). Using portable energy dispersive X-ray fluorescence (EDXRF) analysis for on-site study of ceramic sherds at El Hibeh, Egypt. *Journal of Archaeological Science*, 32, 1613–1623.
- [29] Frahm, E. (2018). Ceramic studies using portable XRF: From experimental tempered ceramics to imports and imitations at Tell Mozan, Syria. *Journal of Archaeological Science*, 90, 12–38.
- [30] Hunt, A. M. W., Speakman, R. J. (2015). Portable XRF analysis of archaeological sediments and ceramics. *Journal of Archaeological Sciences*, 53, 626–638.
- [31] Emmitt, J.J., McAlister, A.J., Phillips, R.S., Holdaway, S.J., (2018). Sourcing without sources: Measuring ceramic variability with pXRF. *Journal of Archaeological Science: Reports*, 17, 422-432.
- [32] Pincé, P., Braekmans, D., Abdali, N., De Pauw, E., Amelirad, S., Vandenaabeele, P. (2018). Development of ceramic production in the Kur River Basin (Fars, Iran) during the Neolithic. A compositional and technological approach using X-ray fluorescence spectroscopy and thin section petrography. *Archaeological and Anthropological Sciences*, 1-18.
- [33] Abzalov, M. (2008). Quality Control of Assay Data: A Review of Procedures for Measuring and Monitoring Precision and Accuracy. *Exploration and Mining Geology*, 17(3-4):131–144.
- [34] Baxter, M. (2003). *Statistics in Archaeology*. London: Hodder Arnold.
- [35] VanDerwarker, A. M. and Marcoux, J. B. (2019). Principal Component Analysis. In *The Encyclopedia of Archaeological Sciences*, S. L. López Varela (Ed.). doi:10.1002/9781119188230.saseas0477
- [36] Braekmans D. and Degryse P. (2016). Petrography: Optical Microscopy. In: A. Hunt (ed.) *The Oxford Handbook of Archaeological Ceramic Analysis*, Oxford University Press, Oxford, p233-265.
- [37] Quinn, P. S. (2013). *Ceramic Petrography: The Interpretation of Archaeological Pottery & Related Artefacts in Thin Section*. Oxford: Archaeopress.
- [38] Weigand P. C., Harbottle G., Sayre, E.V. (1977). Turquoise sources and source analysis: Mesoamerica and the Southwestern USA. In: Earle TK and Ericson JE (eds.), *Exchange Systems in Prehistory* (pp. 15–34). New York: Academic Press.
- [39] Orton, C., & Hughes, M. (2013). *Pottery in Archaeology*. New York: Cambridge University Press.
- [40] Degryse, P., Braekmans, D. (2013). Elemental and Isotopic Analysis of Ancient Ceramics and Glass. In H. H. Turekian, *Treatise on geochemistry (Vols. 2nd Edition, vol. 14, 191-207)*. Oxford: Elsevier.
- [41] Wronkiewicz D. J. and Condie K. C. (1987) *Geochemistry of Archean shales from the Witwatersrand Supergroup, South*

- Africa: Source-area weathering and provenance. *Geochimica et Cosmochimica Acta*, 51, 2401–2416.
- [42] Arnold, D. E. (2000). Does Standardization of Ceramic Pastes Really Mean Specialization? *Journal of Archaeological Method and Theory*, 7, 333–375.
- [43] Gosselain, O. P., Livingston-Smith, A. (2005). The source: Clay selection and processing practices in sub-Saharan Africa. In: Livingston-Smith, Bosquet, A., Martineau, D. (Eds), *Pottery manufacturing processes: reconstitution and interpretation. Acts of the XIVth UISPP Congress, University of Liège, Belgium, 2–8 September 2001*. Oxford: BAR-IS 1349(2005) 33–47.
- [44] Rice, P. M. (1987). *Pottery analysis: A sourcebook*. Chicago: University of Chicago Press.
- [45] Alberio, D. S. (2014). *Materiality, Techniques and Society in Pottery Production: The Technological Study of Archaeological Ceramics Through Paste Analysis*. Warsaw/Berlin: De Gruyter Open Ltd.
- [46] Michelaki, K., Braun, G. V., Hancock, R. G. V. (2015). Local Clay Sources as Histories of Human–Landscape Interactions: a Ceramic Taskscape Perspective. *Journal of Archaeological Method and Theory*, 22(3), 783–827.

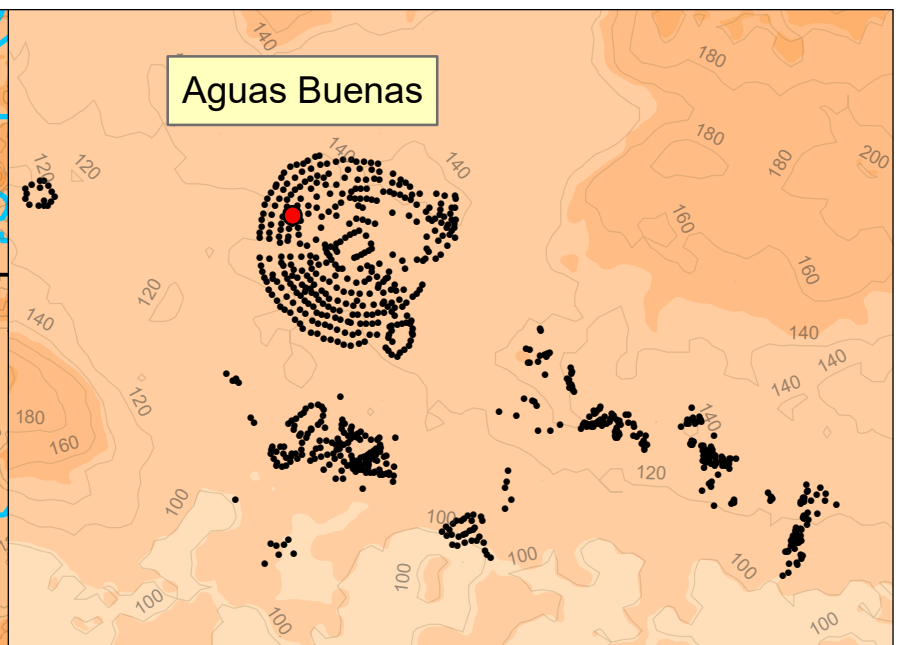
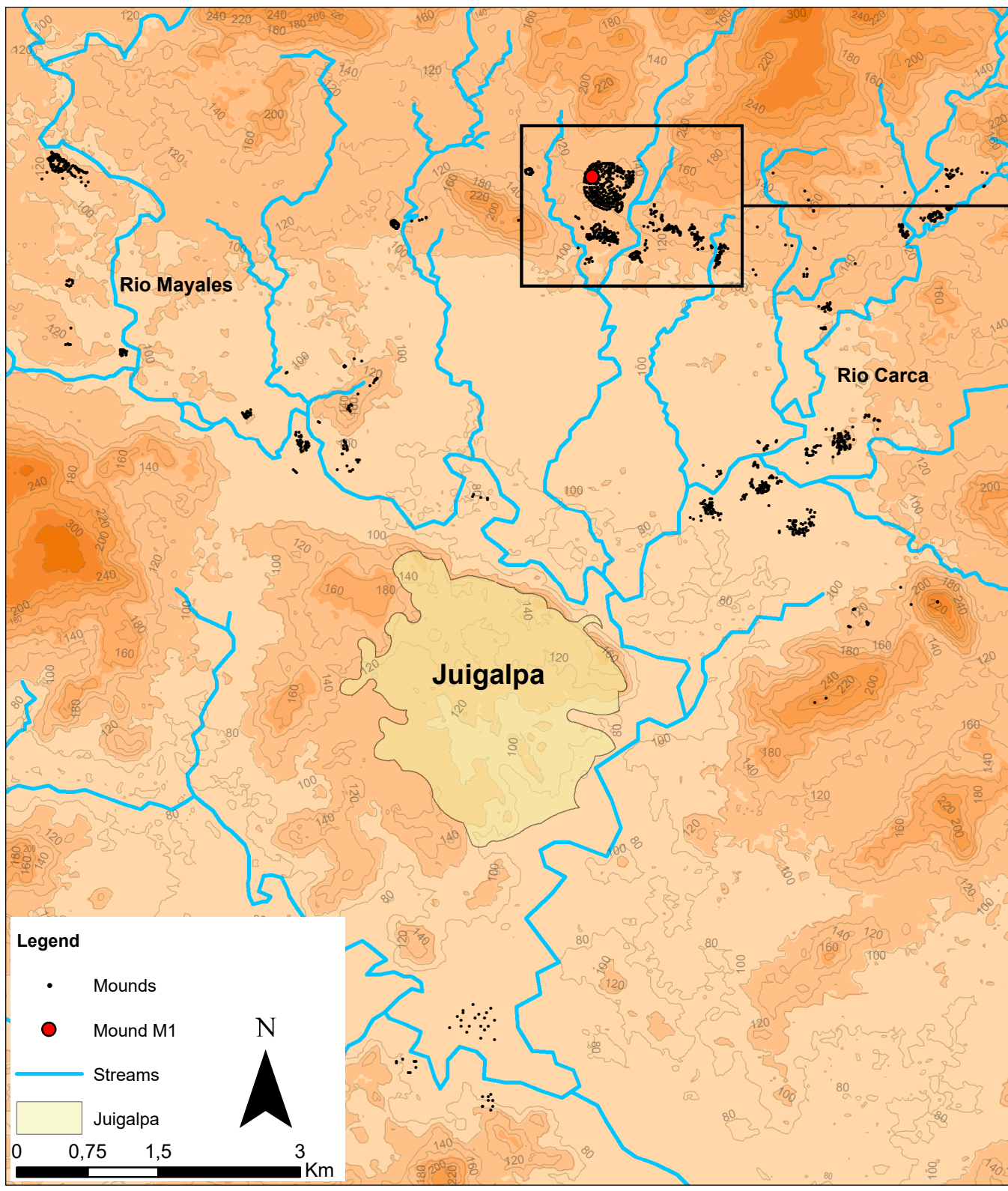
## Figures

Fig.1: Location of the research area in central Nicaragua, highlighting Aguas Buenas.

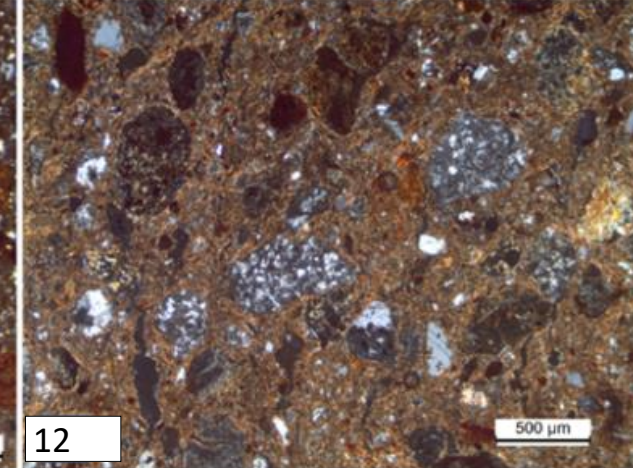
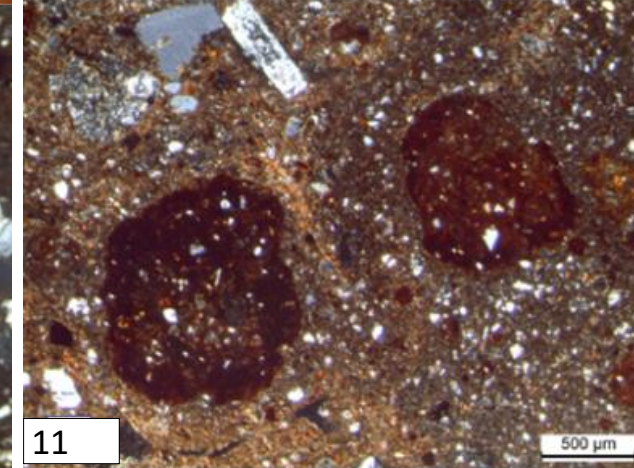
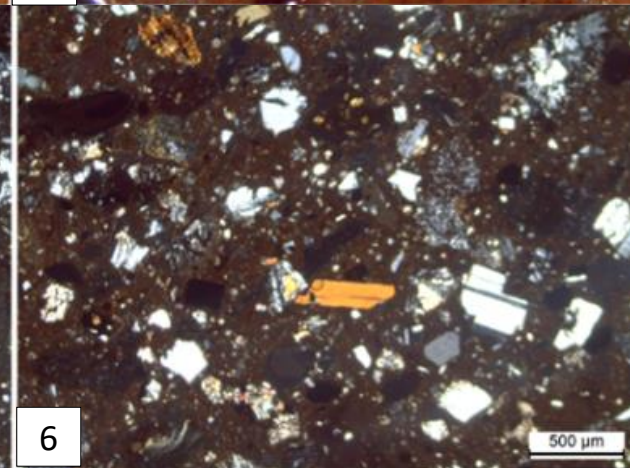
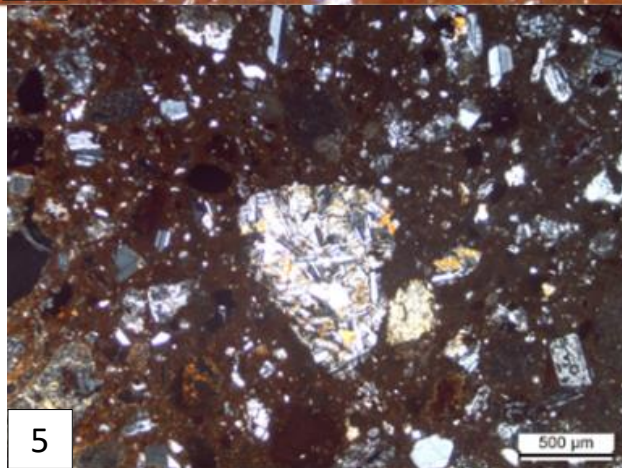
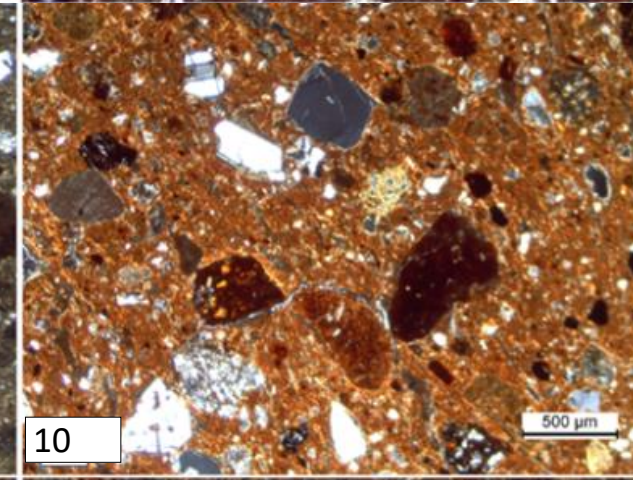
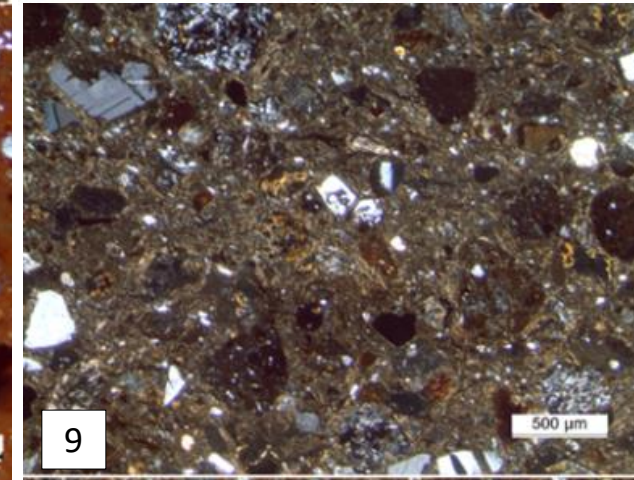
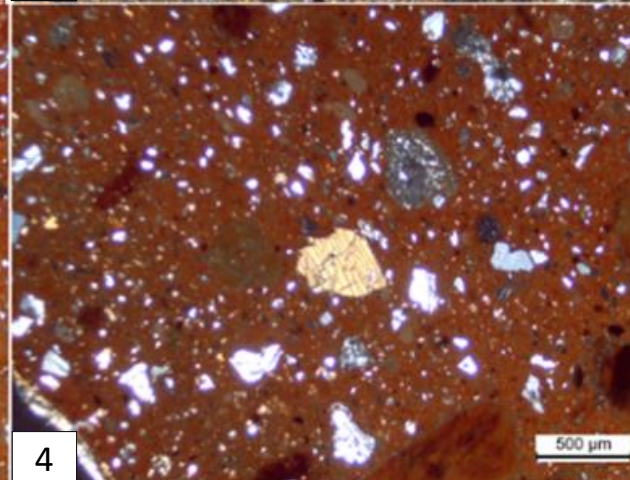
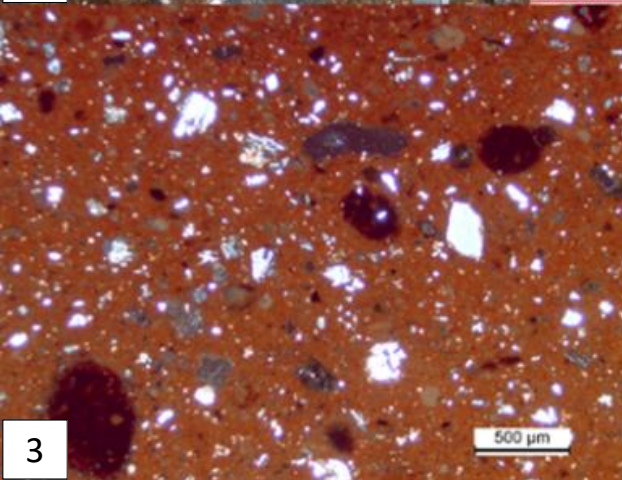
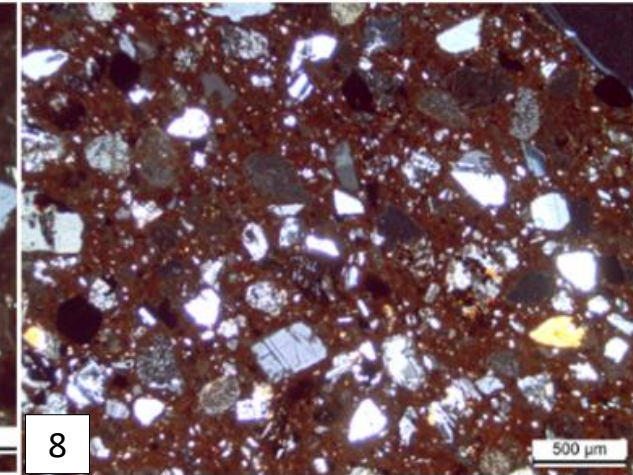
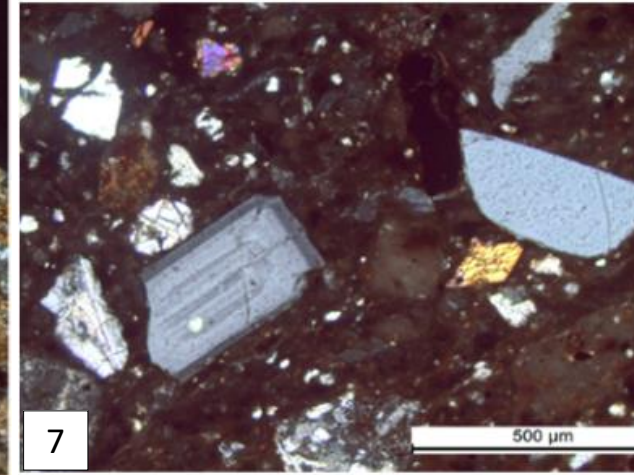
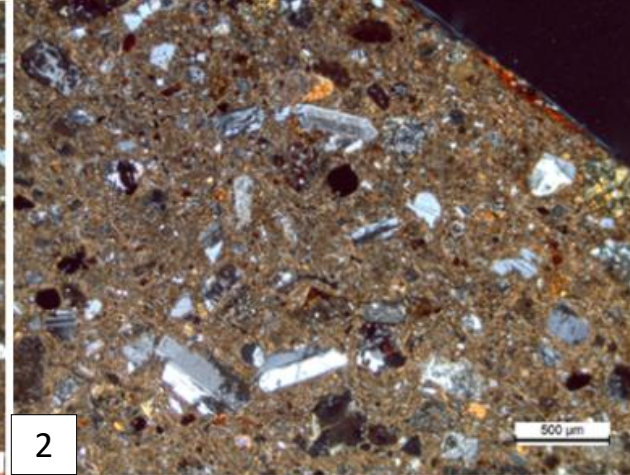
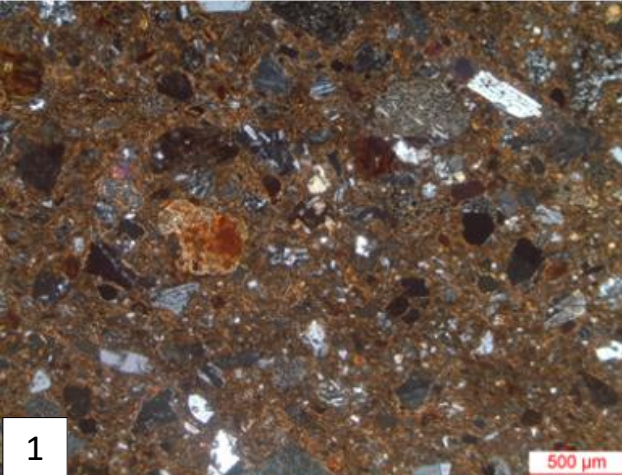
Fig.2: Petrographic groups Chontales A (1 and 2); Chontales B (3 and 4); Chontales C-1(5 and 6); Chontales C-2 (7 and 8); Chontales D-1 9 and 10); Chontales D-2 (11 and 12).

Fig.3: Biplot of CaO (wt.%) vs. Sr (ppm), CaO (wt.%) vs. Zr (ppm) values of the archaeological ceramics from Aguas Buenas M1. Samples are coloured according to the results of the petrographic analysis.

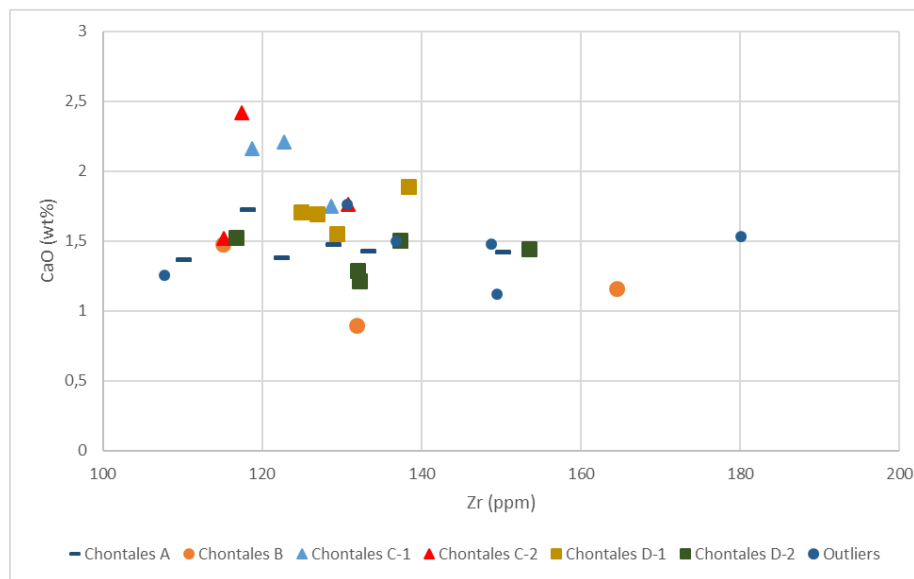
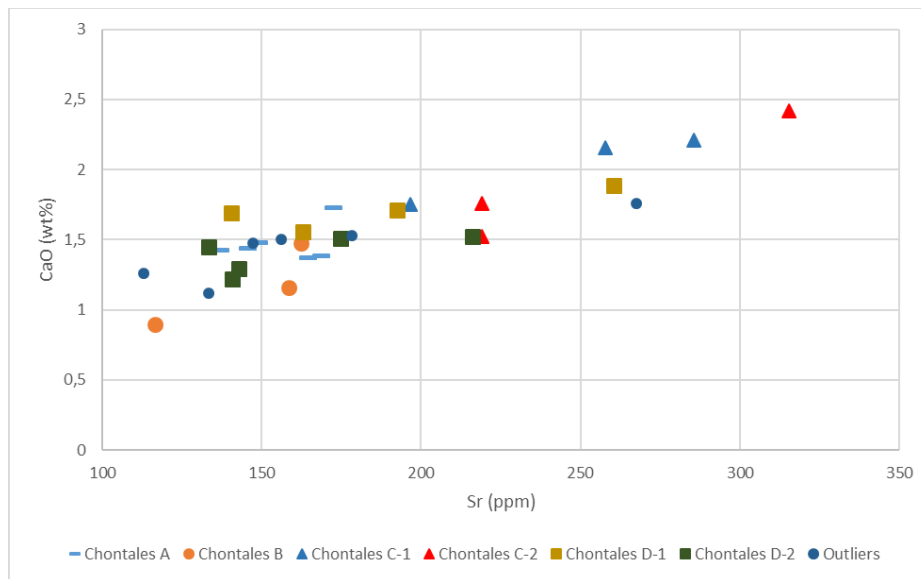
Fig.4: At the top combined PCA results of clay samples and archaeological ceramics. Each colour represents one of the four compositional groups identified with the PCA for clays (Casale et al. [15]) and the six petrographic groups for ceramics. At the bottom Geographic distribution of clay samples associated to Aguas Buenas (red dots) combined with the distribution of mounds (smaller black dots) and different intensities of surface ceramics.











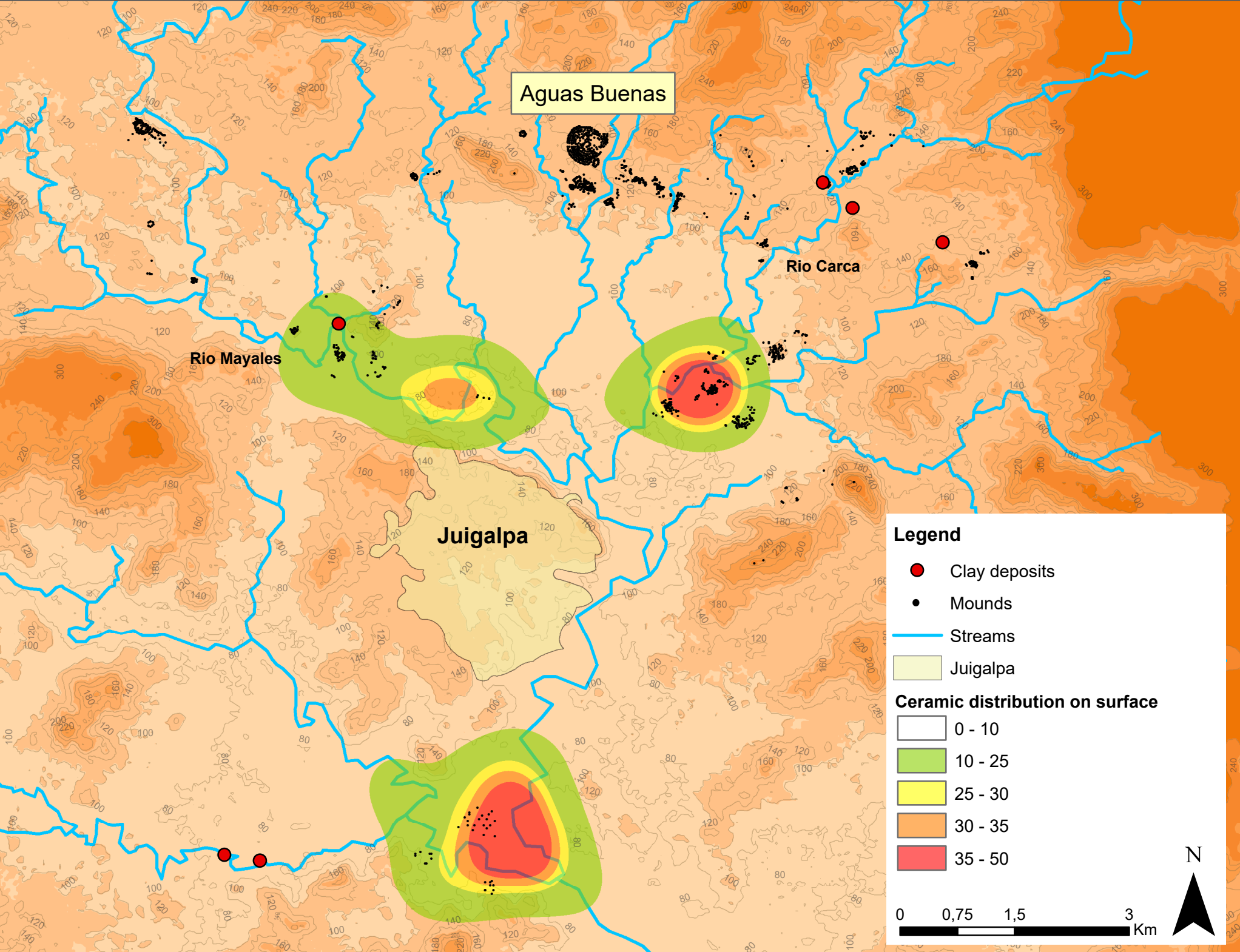
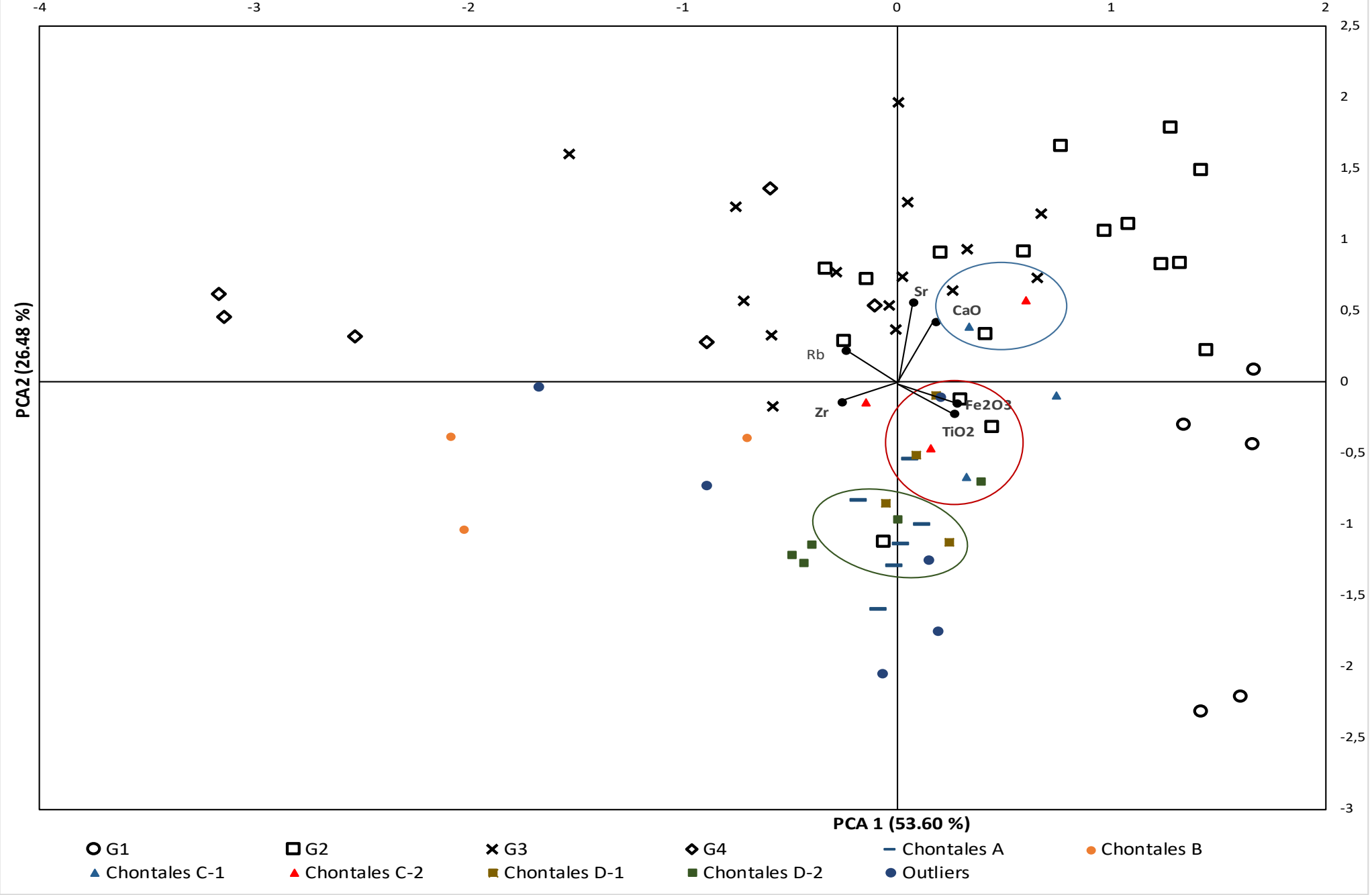




Table 1: Summary of the petrographic analysis.

Group	Chontales A	Chontales B	Chontales C-1	Chontales C-2	Chontales D-1	Chontales D-2
<b>Samples</b>	AB-O-74; AB-C-74A; AB-E-68X; AB-O-71; AB-F-57; AB-I-68; AB- E-71; AB-H-34; AB-P-42; AB-I-74; AB-F-89; AB-I- 83	AB-T-83T; AB-T-60; AB-T-78A	AB-P-71; AB-G-71; AB- M-71; AB-D-78; AB-S- 83P	AB-N-60; AB-A-60; AB- Q-89; AB-G-68; AB-F- 29; AB-A-71Y; AB-M-68	AB-M-83; AB-A-20; AB-A- 71Y; AB-H-78; AB-C-74; AB- I-73	AB-N-45; AB-L- 68; AB-L- 78; AB-B-75; AB-P-24; AB-H-68; AB-N-42
<b>Surface treatment</b>	Absent or minor presence of red line (smoothing) below a post-depositional calcite layer	Traces of light grey post- depositional calcite layers, minimum traces	Traces of light grey post- depositional calcite layers, minimum traces or partly covered	Traces of light grey post- depositional calcite layer	Traces of a post-depositional calcite layer of light grey colour	Traces of a light grey post- depositional layer
<b>Matrix (XP)</b>	Orange-brownish, non- calcareous, microcrystalline.	Dark reddish brown, non- calcareous, optically inactive.	An orange-brown to dark reddish brown non- calcareous, slightly optically active.	A dark brown matrix to dark greyish-brown, non- calcareous. From optically inactive to slightly active.	Light orange-brown	Light yellow-brown matrix, non-calcareous.
<b>General inclusion Size</b>	Significant variation, unsorted, 100 µm up to 600 µm. In a few cases >600 µm	Bi-modal, characterized by fine inclusions <150 µm, and more rarely, medium (150-250 µm). Rare exceptions (500-700 µm)	Significant variation, few from 400-600 µm The common sizes are between 250 to 300 µm few (150-300 µm)	Tri-modal characterized by coarse-medium (300- 600 µm) and medium (150-250 µm)	Unimodal characterized by very coarse inclusions (1000- 2000 µm), coarse (<1 mm) and medium (250-500µm)	Unimodal characterized by medium-coarse (250-800 µm)
<b>Sedimentary rock fragments</b>	Sub-angular and sub rounded chert (300 -500 µm, in a few cases 900- 1000 µm)	Very rare chert +/-110 µm	Sub-angular, sub-rounded and rounded chert (250- 900 µm)	Sub-angular, sub-rounded and rounded chert with significant variation in dimension (isolate 1700 µm; average 200-700 µm)	Sub-angular, sub-rounded and rounded chert (300-1000 µm)	Sub-angular, sub-rounded and rounded chert (300- 1200 µm)
<b>Igneous Rock fragments</b>	Sub-angular and sub- rounded granite, basalt and andesite (150-600 µm)	Sub-rounded and rounded granite (90-120 µm) and few (200-400 µm), rare andesite.	Sub-angular and sub- rounded granite (200-600 µm), few basalt (200-300 µm) and andesite (250- 550 µm)	Sub-angular and sub- rounded granite (200-600 µm) basalt and andesite (150-650 µm)	Sub-angular and sub-rounded granite (200-800 µm), basalt (250-300 µm) and andesite (250-650 µm)	Rare sub-angular and sub- rounded granites (200-900 µm), sub-rounded and rounded large basalt (200 µm- 1.2 mm) and andesite (250-800 µm)
<b>Metamorphic Rock Fragments</b>	n/a	n/a	n/a	n/a	n/a	n/a
<b>Pyroxene (Ortho or clino)</b>	Few orthopyroxene (100- 300 µm) and clinopyroxene (augite 300-150 µm)	Rare clinopyroxene (augite) <90 µm and very rare orthopyroxene <300 µm	Orthopyroxene (100- 300 µm) and clinopyroxene (augite and rare diopside) (200-600 µm)	Ortho (100-350 µm) and frequent clinopyroxene (augite and very rare diopside) (150-300 µm)	Common orthopyroxene (70- 300 µm) and rare clinopyroxene (augite) 150- 300 µm	Rare orthopyroxene (100- 300 µm) and clinopyroxene (augite and (150-400 µm)
<b>Amphibole</b>	Very rare, hornblende (euhedral), (150-300 µm)	n/a	Rare 150-340 µm	Very rare hornblende (100-400 µm).	Very rare	N/a
<b>Mica</b>	Very rare biotite crystals (50-250 µm)	n/a	Very rare biotite of medium dimension (150- 500 µm).	Very rare biotite +/-300 µm.	Very rare	Rare biotite 50-300 µm

<b>Quartz</b>		30% sub-rounded, 70% sub-angular (50-500 µm).	50% sub-rounded, 50% sub-angular (130-50 µm) and few (150-200 µm).	30% sub-rounded, 70% sub-angular, (700-300 µm)- (50-200 µm).	% sub rounded 30 %sub-angular 70 (50-500 µm)	30% sub-rounded, 70% sub-angular, (50-500 µm)	30% sub-rounded, 70 %sub-angular, (300-650 µm) -(50-250 µm).
<b>Heavy minerals</b>		Angular, sub-angular and sub-rounded (100-300 µm).	Rounded, sub-rounded and sub-angular (50-80 µm).	Sub-rounded and sub-angular (100-300 µm).	Sub-rounded and sub-angular (80-400 µm).	Rounded, sub-rounded and sub angular (90-350 µm).	Sub-rounded and sub-angular (100-300 µm).
<b>K-feldspars</b>		K-feldspars and plagioclase (150-500 µm), rare sanidine (450 µm).	K-feldspars and plagioclase, euhedral shape, angular and sub angular (50-250 µm).	K-feldspars and plagioclase, angular and sub angular. (100-450 µm).	K-feldspars and plagioclase (100-700 µm), angular and-sub angular.	K-feldspars and plagioclase, rare sanidine euhedral shape, angular and sub-angular. (150-600 µm).	K-feldspars and plagioclase (few large 700-1500 µm; average 150-500 µm), sanidine (700-1000), angular .and sub angular.
<b>Olivine</b>		Rare olivine (50-300 µm) and very rare iddingsite (100-150 µm).	Rare, +/- 50 µm.	Few, 50-250 µm; rare iddingsite.	Few, 50-300 µm.	Rare 150-500 µm.	Few, 50-400 µm.
<b>Unknown</b>		Hydrothermal alteration (150-350 µm).	Powdered granite with micropheno-crystals of olivine.	From no to rare hydrothermal alteration (200-250 µm).	Some cases of powdered granite with micropheno-crystals of olivine and hydrothermal alteration.	Hydrothermal alteration, in some cases in oolite shape. Powdered granite with micropheno-crystals of olivine.	Some cases of hydrothermal alteration (250-350 µm) and very rare powdered granite with micropheno-crystal of olivine.
<b>Clay pellets</b>		Rounded and sub-rounded clay pellets in various amounts (250-1300 µm).	Rounded clay pellets of significance dimensions (1,7 mm- 300 µm-750 µm).	Rare rounded and sub-rounded, 300-400 µm.	Rare rounded and sub-rounded (rare +/- 1.3mm and average 300-400 µm).	Rare rounded and sub-rounded, 200-700 µm.	N/a
<b>Grog</b>		Rare or not present (700 µm-2000 µm).	An isolate case in one sample, 600 µm.	From very rare to no examples (300-400 µm).	n/a	Few large grog fragments (400 µm -1500 µm).	Few large grog fragments (1100-1600 µm) and (400-500 µm).
<b>Porosity</b>		Mostly elongated voids, moderately oriented with the borders.	Long elongated voids and voids are both orientated with the borders.	Elongated, vugh and vesicle pores moderately oriented with the borders.	Elongated, vugh and vesicle pores, from moderately oriented with the borders to not oriented.	Elongate, vugh and vesicle pores from not oriented to moderately oriented.	Elongate, vughs and vesicles pores, moderately oriented with the borders.
	<b>Approx. Void Size (µm)</b>	150-250 µm.	100-200 µm and some large cracks (600 µm-2000-3000 µm).	50-250 µm.	50-250 µm.	50-250 µm.	50-250 µm, in a few cases large 300-400 µm.
	<b>%paste</b>	65-70%	80%	60-65%	60-65%	65-70 %	65-70%

Table 2: pXRF results of archaeological ceramics.

Macroscopic group	Group	Sample	CaO (wt%)	Fe <sub>2</sub> O <sub>3</sub> (wt%)	TiO <sub>2</sub> (Wt%)	Sr (ppm)	Cr (ppm)	Zr (ppm)	Rb (ppm)	Nb (ppm)
AB-O	Chontales A	AB-O-71	1,4	9,1	1,2	137	n.d.	150	53	< 5
AB-C	Chontales A	AB-C-74A	1,4	10,3	1,3	164	73	110	61	< 5
AB-E	Chontales A	AB-E-68X	1,4	11,5	1,3	145	213	133	60	< 5
AB-F	Chontales A	AB-F-57	1,7	10,4	1,4	172	28	118	66	< 5
AB-O	Chontales A	AB-O-74	1,5	12,0	1,4	149	1	129	64	< 5
AB-I	Chontales A	AB-I-83	1,4	11,2	1,2	169	134	122	65	< 5
AB-T	Chontales B	AB-T-60	1,5	5,3	1,0	162	14	115	63	< 5
AB-T	Chontales B	AB-T-78A	0,9	3,1	0,8	117	35	132	70	< 5
AB-T	Chontales B	AB-T-83Q	1,2	3,3	0,7	159	127	165	68	< 5
AB-G	Chontales C-1	AB-G-71	2,2	9,9	1,3	286	16	123	61	< 5
AB-M	Chontales C-1	AB-M-71	1,8	11,3	1,4	197	145	129	60	< 5
AB-P	Chontales C-1	AB-P-71	2,2	10,8	1,6	258	96	119	57	< 5
AB-Q	Chontales C-2	AB-Q-89	1,8	9,6	1,1	219	n.d.	131	64	< 5
AB-N	Chontales C-2	AB-N-60	1,5	9,9	1,3	219	123	115	61	< 5
AB-A	Chontales C-2	AB-A-60	2,4	10,5	1,5	315	14	117	62	< 5
AB-D	Chontales D-1	AB-A-20	1,7	12,1	1,6	141	59	127	64	< 5
AB-A	Chontales D-1	AB-A-71Y	1,6	11,5	1,2	163	132	129	64	< 5
AB-M	Chontales D-1	AB-M-83	1,7	10,3	1,3	192	112	125	62	< 5
AB-H	Chontales D-1	AB-H-78	1,9	10,9	1,3	260	23	138	61	< 5
AB-B	Chontales D-2	AB-B-75	1,5	11,1	1,3	175	14	137	61	< 5
AB-H	Chontales D-2	AB-H-68	1,5	10,8	1,4	216	n.d.	117	58	< 5
AB-L	Chontales D-2	AB-L-68	1,2	10,7	1,1	141	76	132	66	< 5
AB-L	Chontales D-2	AB-L-78	1,3	10,6	1,3	143	84	132	69	< 5
AB-N	Chontales D-2	AB-N-45	1,4	10,3	1,2	133	39	153	66	< 5
AB-R	AB-R-74	AB-R-74	1,3	11,2	1,4	113	229	108	60	< 5
AB-S	AB-S-78	AB-S-78	1,8	10,7	1,3	268	213	131	61	< 5
AB-E	AB-E-68Y	AB-E-68Y	1,5	6,0	0,7	178	37	180	71	< 5
AB-F	AB-F-29	AB-F-29	1,1	11,0	1,3	133	30	149	54	< 5
AB-D	AB-D-29	AB-D-29	1,5	12,0	1,5	156	145	137	61	< 5
AB-D	AB-D-45	AB-D-45	1,5	7,2	0,9	147	76	149	64	< 5

Standard deviation	CaO (wt%)	CaO (st. dev)	Fe <sub>2</sub> O <sub>3</sub> (wt%)	Fe <sub>2</sub> O <sub>3</sub> (st. dev)	TiO <sub>2</sub> (wt%)	TiO <sub>2</sub> (st. dev)	Sr (ppm)	Sr (st. dev)	Cr (ppm)	Cr (st. dev)	Zr (ppm)	Zr (st. dev)	Rb (ppm)	Rb (st. dev)	Nb (ppm)	Nb (st. dev)
Chontales A	1,5	0,1	10,8	0,9	1,3	0,1	156	13,0	69	77,1	127	12,7	62	4,4	< 5	0,5
Chontales B	1,2	0,2	3,9	1,0	0,9	0,1	145	20,7	58	48,9	137	20,5	67	3,0	< 5	1,7
Chontales C-1	2,0	0,2	10,7	0,6	1,4	0,1	246	37,2	85	53,2	123	4,1	60	1,7	< 5	0,5
Chontales C-2	1,9	0,4	10,0	0,4	1,3	0,1	251	45,4	29	55,0	121	6,9	62	1,4	< 5	0,9
Chontales D-1	1,7	0,1	11,2	0,7	1,3	0,1	189	45,1	81	43,2	129	5,2	63	1,4	< 5	0,5
Chontales D-2	1,4	0,1	10,7	0,3	1,3	0,1	162	30,8	35	33,1	134	11,8	64	4,1	< 5	0,7

Table 3: Average and standard deviation for the petrographic groups.

Type of soil	Group	Sample	Petrographic group connections	CaO (wt%)	Fe <sub>2</sub> O <sub>3</sub> (wt%)	TiO <sub>2</sub> (Wt%)	Cr (ppm)	Sr (ppm)	Zr (ppm)	Rb (ppm)	Nb (ppm)	UTM_(E)	UTM_(N)	Visible Estimated Outcrop (m)	Sample Depth (m)
Arenoso/Barro	G1	ZA.1		4,8	16,8	2,2	295	160	112	62	7	672376	1342189	50x50	0,5-2
Barro_negro	G1	ZA.2		3,5	15,8	1,9	261	145	104	63	6	672862	1344023	1x10	0,2-0,5
Barro_amarillo	G1	ZA.3		3,4	15,5	2,0	234	158	99	56	7	672925	1343965	-	-
Barro_negro	G1	ZA.6		1,8	17,9	2,4	313	105	118	53	7	672925	1343965	-	-
Barro	G1	ZA.7		2,1	18,6	2,3	325	91	106	53	7	672774	1344018	-	-
Barro	G2	C3.1		2,1	9,5	1,1	152	308	130	67	< 5	674038	1334509	0x5	1
Barro	G2	D12.1	Chontales C-1, Chontales C-2	2,3	9,8	1,0	136	221	97	59	< 5	673761	1343369	3x10	>0,3
Barro_amarillo	G2	F12.3		2,3	10,0	1,2	103	368	127	64	< 5	673395	1341787	10x15	>1
Barro	G2	F4.1		2,6	11,4	1,3	155	305	78	58	< 5	674499	1334435	1x30	0-1,5
Barro	G2	F6.1		2,3	9,0	1,0	123	276	135	69	< 5	675376	1341229	10x20	2
Barro	G2	F6.3		2,6	11,3	1,2	279	333	108	63	< 5	674850	1341220	20x20	>0,2
Barro	G2	G6.1		2,6	9,8	1,1	358	445	81	64	< 5	675534	1341463	20x40	>0,3
Arenoso/Barro	G2	H2.2		2,6	11,9	1,2	143	353	88	60	< 5	677013	1334541	-	-
Barro_negro	G2	H2.3		2,8	12,2	1,2	164	329	81	61	< 5	676812	1334640	-	-
Barro	G2	H3.1		3,3	12,7	1,4	327	402	79	60	< 5	676962	1342742	5x400	>1
Barro	G2	H3.2		2,5	13,6	1,6	458	376	87	60	< 5	677206	1340460	25x25	5-6m
Arenoso/Barro	G2	H5.1		3,5	11,2	1,3	279	457	86	60	< 5	677347	1340986	30x2	-
Barro_negro	G2	I11.1		2,2	14,1	1,3	390	267	73	56	< 5	677641	1335321	10x10	0,5
Barro/Barrial	G2	M3.1	Chontales C-2, Chontales D-1, Chontales D-2	1,9	11,0	1,2	123	192	99	66	< 5	677640	1335322	10x10	0,5-0,7
Barro	G2	M3.2	Chontales A, Chontales D-1, Chontales D-2	1,4	12,7	1,3	171	129	109	69	< 5	677481	1340619	2x5	1
Barro	G2	N3.1		1,9	10,0	1,1	216	221	117	71	< 5	679278	1344248	-	-
Barro	G2	N4.2	Chontales C-2, Chontales D-1, Chontales D-2	2,3	9,1	1,1	141	149	96	57	< 5	679323	1344707	-	-
Barro/Barrial	G3	B2.4		2,1	3,9	0,6	26	382	173	66	< 5	679071	1343650	2x3	0,5-1
Arenoso/Barro	G3	C12.1	Chontales C-1, Chontales C-2	2,5	9,2	1,0	46	264	89	58	< 5	679143	1343647	2x10	0,5-1
Barro	G3	C5.1		2,2	7,0	1,0	37	347	154	72	< 5	678730	1341642	50x50	2

Barro	G3	D5.1		2,5	8,4	1,1	35	337	111	69	< 5	678738	1339413	5x10	-
Barro	G3	D5.2		1,9	10,0	1,2	37	296	122	69	< 5	680115	1345503	10x30	0,2-1
Barro	G3	E5.1	Chontales C-1, Chontales C-2	2,0	9,9	1,2	68	337	115	63	< 5	680170	1339736	1x2	1
Barro_amarillo	G3	F12.1		2,4	10,0	1,2	35	352	117	63	< 5	680168	1339732	2x10	1
Barro	G3	G11.2		2,3	9,9	1,1	69	272	138	71	< 5	680280	1339717	2x10	1
Barro	G3	H7.1		2,4	9,4	1,2	n.d.	308	138	64	< 5	680915	1341320	10x20	0-1
Barro	G3	I7.1		2,0	7,8	0,9	84	227	132	73	< 5	680719	1339423	5x10	0,2-1,2
Barro	G3	I7.2		2,0	8,0	1,0	73	194	127	72	< 5	682161	1344172	5x10	0,25-0,6
Barro	G3	L5.2		3,4	8,4	1,0	64	312	99	76	< 5	681898	1343234	100x100	0,1-0,2
Barro	G3	L7.1		1,8	10,6	1,2	75	252	108	72	< 5	681871	1343310	50x50	0,20-0,40
Barro	G3	M2.1		2,6	10,3	1,1	68	337	89	62	< 5	683424	1343871	10x50	> 0,3
Barro/Barrial	G3	O5.1		1,6	8,3	1,1	14	218	143	66	< 5	683436	1342528	1x10	0,25
Barro	G4	A4.2		2,3	5,8	1,2	n.d.	417	153	69	< 5	684135	1341858	2x10	0,2-0,25
Barro	G4	B2.5		1,6	3,9	0,4	n.d.	127	204	88	< 5	623088	1300805	0,5x1	0,4
Barro	G4	B2.6		1,3	3,9	0,5	n.d.	190	195	73	< 5	624006	1301271	0,5x10	0,2
Barro	G4	B2.7		1,7	3,6	0,5	n.d.	129	213	96	< 5	624094	1301410	0,5x2	0,1
Barro_amarillo	G4	G11.3		2,3	9,9	1,2	n.d.	267	138	69	< 5	623995	1300892	1x10	0,2-0,6
Barro	G4	I7.3		1,5	8,4	1,1	n.d.	243	142	78	< 5	624119	1301006	0,5x5	0,1-0,5

Table 4: p-XRF results for clay samples expressed in wt.% and ppm, together with the geographical coordinates (UTM, WGS84), extension and depth expressed in meter for each clay outcrop, list of the clay samples clustered in groups according to PCA [15], and list of the petrographic groups of archaeological ceramics clustered to clay outcrops according to PCA.

### **Declaration of interests**

☐ The authors declare that they have no known competing financial interests or personal relationships that could have appeared to influence the work reported in this paper.

☐ The authors declare the following financial interests/personal relationships which may be considered as potential competing interests:

--

#### Credit author statement

Simone Casale: Conceptualization, Investigation, Formal analysis, Writing- Original draft preparation, Visualization, data curation, Methodology

Natalia Donner: conceptualization, Formal analysis, Methodology

Dennis Braekmans: Methodology, Supervision, Resources, Data Curation

Alex Geurds: Funding acquisition, Project administration, Supervision



### Supplementary tables

**Table S1** : Certified versus measured values of reference materials. including percent relative difference (% RD) (n.d. not determined).

	<b>98b</b>			<b>GSP-2</b>			<b>BIR-1a</b>			<b>CRM667</b>			<b>SGR-1b</b>		
	certified	measured	% RD	certified	measured	% RD	certified	measured	% RD	certified	measured	% RD	certified	measured	% RD
K <sub>2</sub> O (wt.%)	3.38	3.46	2.41	5.38	5.11	5.06	0.03	n.d.	-	n.d.	-	-	1.66	1.8	7.89
CaO (wt.%)	0.11	0.14	25.88	2.1	1.9	10.26	13.3	12.46	6.48	n.d.	-	-	8.38	8.95	6.54
TiO <sub>2</sub> (wt.%)	1.35	1.41	4.42	0.66	0.67	1.77	0.96	1.02	6.51	n.d.	-	-	0.24	0.27	13.01
Fe <sub>2</sub> O <sub>3</sub> (T) (wt.%)	1.69	1.59	5.79	4.9	4.52	8.11	11.3	10.81	4.44	6.41	6.58	2.68	3.03	3.09	1.9
Zn (ppm)	110	103	6.49	120	111	7.51	70	68	2.24	175	141	21.2	74	83	11.97
Ni (ppm)	n.d.	-	-	17	13	27.14	170	117	37.13	128	143	11.16	29	31	6.88
Rb (ppm)	180	178	1.24	245	230	6.35	n.d.	-	-	n.d.	-	-	n.d.	-	-
Sr (ppm)	189	195	3.06	240	226	5.95	110	112	2.06	206-243	204	8.66	420	410	2.32
Y (ppm)	n.d.	-	-	28	n.d.	-	16	-	-	16.7-25.3	-	-	13	-	-
Zr (ppm)	220	231	4.89	550	517	6.24	18	14	23.78	n.d.	-	-	53	55	3.2
Nb (ppm)	n.d.	-	-	27	24	9.99	0.6	-	-	n.d.	-	-	5	-	-
Cr (ppm)	119	127	6.82	20	23	14.37	370	352	5.08	178	190	6.52	30	34	11.1

**Table S2** Number of cases predicted and assigned to each of the petrographic groups based on discriminant analysis using Mahalanobis distances.

Classification Results: 79.2% of original grouped cases correctly classified.									
Groups			Predicted Group Membership						Total
			1	2	3	4	5	6	
Original	Count	1 - Chontales A	5	0	0	0	0	1	6
		2 - Chontales B	0	3	0	0	0	0	3
		3 - Chontales C-1	0	0	1	1	1	0	3
		4 - Chontales C-2	0	0	1	2	0	0	3
		5 - Chontales D-1	1	0	0	0	3	0	4
		6 - Chontales D-2	0	0	0	0	0	5	5
	%	1 - Chontales A	83.3	0	0	0	0	16.7	100
		2 - Chontales B	0	100	0	0	0	0	100
		3 - Chontales C-1	0	0	33.3	33.3	33.3	0	100
		4 - Chontales C-2	0	0	33.3	66.7	0	0	100
		5 - Chontales D-1	25	0	0	0	75	0	100
		6 - Chontales D-2	0	0	0	0	0	100	100

**Table S3** Ceramic and clay samples grouped according to PCA and the predicted groups following the DA analysis. Statistical differences for group attribution are indicated with \*\*.

Sample code	Prior PCA group	Predicted DA group		Sample code	Prior PCA group	Predicted DA group
ZA.1	1	1		<b>F12.1</b>	<b>3</b>	<b>2**</b>
Za.2	1	1		G11.2	3	3
ZA.3	1	1		<b>H7.1</b>	<b>3</b>	<b>5**</b>
ZA.6	1	1		I7.1	3	3
ZA.7	1	1		I7.2	3	3
<b>C3.1</b>	<b>2</b>	<b>3**</b>		L5.2	3	3
D12.1	5	5		L7.1	3	3
F12.3	2	2		<b>M2.1</b>	<b>3</b>	<b>2**</b>
<b>F6.1</b>	<b>2</b>	<b>3**</b>		<b>O5.1</b>	<b>3</b>	<b>7**</b>
F6.3	2	2		A4.2	4	4
G6.1	2	2		B2.5	4	4
H2.2	2	2		B2.6	4	4
H2.3	2	2		B2.7	4	4
H3.2	2	2		<b>G11.3</b>	<b>4</b>	<b>3**</b>
H5.1	2	2		I7.3	4	4
M3.2	6	6		<b>AB-C-74A</b>	<b>6</b>	<b>7**</b>
<b>N3.1</b>	<b>2</b>	<b>3**</b>		AB-E-68X	6	6
N4.2	7	7		AB-O-74	6	6
<b>F4.1</b>	<b>2</b>	<b>5**</b>		AB-I-83	6	6
H3.1	2	2		AB-G-71	5	5
I11.1	2	2		AB-N-60	7	7
M3.1	7	7		AB-A-60	5	5
<b>B2.4</b>	<b>3</b>	<b>4**</b>		AB-A-20	6	6
C12.1	5	5		AB-A-71Y	6	6

C5.1	3	3		AB-M-83	7	7
D5.1	3	3		<b>AB-H-78</b>	<b>7</b>	<b>5**</b>
D5.2	3	3		AB-B-75	6	6
<b>E5.1</b>	<b>5</b>	<b>3**</b>		<b>AB-L-68</b>	<b>7</b>	<b>6**</b>